

ECOLOGY | ARTICLE

The effect of single versus successive warm summers on an intertidal community

Amelia V. Hesketh^{1,2*}, Cassandra A. Konecny², Sandra Emry², and Christopher D. G. Harley^{2,3}

Author affiliations:

1. School of Resource and Environmental Management, Simon Fraser University, Burnaby, BC, Canada
2. Department of Zoology, University of British Columbia, Vancouver, BC, Canada
3. Institute for the Oceans and Fisheries, University of British Columbia, Vancouver, BC, Canada

* Corresponding author: ahesketh@sfu.ca

OPEN RESEARCH STATEMENT:

Data are archived in Zenodo: <https://doi.org/10.5281/zenodo.15054128>. Code is also archived in Zenodo: <https://doi.org/10.5281/zenodo.15054111>.

KEYWORDS: barnacles; climate change; community; diversity; foundation species; heatwaves; intertidal zone; mortality; repeated stressors; warming

ABSTRACT

To accurately predict how organisms and ecological communities will respond to future conditions caused by climate change, we must consider the temporal dynamics of environmental stressors, including the effects of repeated exposures to stress. We performed a two-year passive thermal manipulation in coastal British Columbia, Canada to determine how intertidal communities responded to single and successive warm summers. Warm temperatures had both negative contemporaneous effects within years and persistent negative effects across years. Warming reduced organism densities, altered population dynamics, and affected community structure and diversity, patterns which were likely mediated by differences in foundation species (barnacle) abundance between treatments. Unexpectedly, the effects of thermal stress in the second year were rarely dependent on whether temperatures were warm during the first year. Our study suggests that, while this intertidal community can recover from single warm summers, recurring thermal stress has additive negative effects, resulting in a more depauperate, less diverse community over time, particularly if foundation species are negatively affected.

INTRODUCTION

Just as global mean surface temperatures are expected to increase over the coming decades (IPCC 2023), so, too, are the frequency, severity, and duration of extreme temperature events such as heatwaves (Oliver et al. 2018, Perkins-Kirkpatrick and Lewis 2020). Extreme temperatures have biological consequences. Heatwaves increase the probability of environmental temperatures surpassing the thermal optima and maxima of organisms (Vasseur et al. 2014). Thus, heatwaves can impair fitness (Siegle et al. 2022) and, ultimately, cause mortality for thermally sensitive species (Harley 2008, Hesketh and Harley 2023), with ramifications for

populations, communities, and ecosystems (Harris et al. 2018; Montie and Thomsen 2023).

The effects of heatwaves on organisms are increasingly well-studied; however, the consequences of repeated exposures to thermal stress have received less attention. Thermal stress events that are prolonged or occur in rapid succession can exert stronger negative effects on organism survival and fitness (Ma et al. 2018; Siegle et al. 2022). However, responses vary among species — for species with acclimatory capacity, prior exposure to thermal stress may engender resilience to subsequent heatwaves, while for those without, the negative effects of repeated heatwaves may instead accumulate (Pansch et al. 2018). At the community level, for which controlled warming manipulations can be experimentally challenging and studies are correspondingly limited, repeated heatwaves have resulted in communities that are more depauperate (Dal Bello et al. 2019) and homogenous (Hammill and Dart 2022). However, community-level resilience to thermal stress may increase with repeated exposures as thermally sensitive species are eliminated and thermally tolerant species survive (Hughes et al. 2019). Manipulating the timing of thermal stress events is an important additional step towards understanding their ecological effects.

While environmental extremes affect organisms, the reverse is also true. Foundation species, abundant species that physically structure ecological communities, often create environmentally benign microhabitats for associated organisms (e.g., through moisture retention and shading; Hesketh et al. 2021, Lee et al. 2021, Jurgens et al. 2022, Gutiérrez et al. 2023). The loss of foundation species can thus profoundly impact communities by disrupting interspecific facilitative relationships (Hesketh and Harley 2023; Montie and Thomsen 2023). The importance of such facultative facilitations for bolstering organism survival and performance often increases with environmental stress, though there may be an upper limit beyond which stress cannot be

effectively buffered (Bulleri et al. 2016).

Intertidal organisms are regularly exposed to stressors including hydrodynamic forces, desiccation, and seasonally hot and cold air temperatures. In this highly variable, physiologically taxing environment, foundation species may play an outsized role in attenuating stress and supporting biodiversity. While many intertidal species act as foundation species (e.g., bed-forming bivalves, tunicates, macroalgae, and vascular plants), here, we focus on acorn barnacles. Acorn barnacles are cosmopolitan organisms that facilitate a relatively diverse intertidal community (Harley 2006, Hesketh et al. 2021). Barnacles can retain moisture (Vermeij 1978, Harley and O’Riley 2011), thereby reducing desiccation stress for closely associated species when present at high densities. However, thermal stress can increase barnacle mortality and reduce barnacle abundance (Little et al. 2021; Hesketh and Harley 2023). While empty barnacle tests provide humid, thermally benign microhabitats for other species (Barnes 2000), such habitats are ultimately ephemeral. Barnacle mortality events and recruitment failures, by reducing available habitat, significantly impact the abundance, identity, and diversity of associated organisms (Kordas et al. 2015, Hesketh and Harley 2023).

Here, we tested the effect of single and successive warm summers on high intertidal barnacle bed communities (Fig. 1a) through a two-year passive thermal manipulation using black (warm) and white (cool) settlement tiles (Fig. 1b; Kordas et al. 2015). To manipulate the temporal dimension of thermal stress, the treatments (color) of half of the tiles were swapped after one year. We hypothesized that: H1) because elevated temperatures can reduce organism performance and increase mortality, communities within the warm treatments would have lower invertebrate abundance, algal cover, and alpha diversity than those within cool treatments; H2) warming during the first year, because of its negative contemporaneous effects on foundation

species cover, would exert persistent indirect negative effects during the second year; and H3) the effects of warming in the second year of study would be stronger in communities that were previously exposed to warming due to pre-existing reductions in foundation species cover, and thus reduced availability of thermal refugia (i.e., a positive interaction of warming across years; Fig 1b).

MATERIALS AND METHODS

Site description

This study was completed near TESNO,EN (Beaver Point), a site that lies within the traditional, unceded territory of the WSÁNEĆ peoples in what is now known as Ruckle Provincial Park on Salt Spring Island, British Columbia, Canada (48.77324, -123.36637). The substratum at this site is dominated by a southeast-facing semi-exposed sandstone bench, and tides are mixed semi-diurnal. Relative to the rest of British Columbia's Southern Gulf Islands, this area is exposed to cooler, more saline water and larger waves due to its proximity to Haro Strait and the Strait of Juan de Fuca. However, like these and the neighboring San Juan Islands (USA), the intertidal zone at this site is considered a thermal "hot spot" due to its summertime midday low tides coupled with relatively clear, sunny weather (Helmuth et al. 2006).

Here, the upper intertidal zone is dominated by the acorn barnacles *Balanus glandula* and *Chthamalus dalli*, with sporadic beds of the perennial brown alga *Fucus distichus*. Filamentous ephemeral algae (predominantly the green algae *Ulothrix* sp. and *Urospora* sp.) occur as early colonizers of bare space and foliose ephemeral algae (predominantly *Ulva* spp., *Pyropia* sp., and *Petalonia fasciata*) occur in winter, often attached to underlying barnacles. Dominant herbivores include the littorine snails *Littorina scutulata* and *Littorina sitkana* and the limpets *Lottia*

paradigitalis and *Lottia digitalis*, which tend to migrate down shore with the onset of daytime low tides in spring and return to higher tidal elevations in August (Kordas et al. 2015).

Study design

Individual settlement tiles were built based on previous methods (Kordas et al., 2015; see Appendix S1). In brief, each 15x15 cm tile consisted of a central epoxy settlement surface (6.9x6.9 cm, < 5 mm high Sea Goin' Poxo Putty; Permalite Plastics, USA) bordered by either white (cool treatment) or black (warm treatment) high-density polyethylene (6.4 mm thick; Redwood Plastics, Canada). Temperature differences were driven by the differential absorption of incoming solar radiation during daytime summer low tides. These settlement tiles were affixed to a bottom tile unit composed of thicker white high-density polyethylene (9.5 mm thick; Redwood Plastics, Canada) that was used to anchor the assembly to the underlying bedrock.

This study followed a randomized block design, with six blocks consisting of eight black and eight white tiles ($n = 48$). Tiles were initially installed on 12 April 2019. Some were relocated in June 2019 to avoid disturbance from wave-cast logs, resulting in a final shore level of 2.34 ± 0.07 m (mean \pm SE) above Canadian chart datum. In May 2019, we enclosed tiles with copper "fences" to manipulate grazer diversity and densities (see Appendix S1). We ceased manipulations in August 2019 because wave action, more so than we, controlled littorine snail densities and high summer temperatures caused mortality for limpets, which were prevented from accessing thermal refugia by copper fences. On 3 April 2020, we randomly selected and switched the colour of half of each treatment within each block using white and black heavy-duty tape (Gorilla Tape; Gorilla Glue, Inc., USA; adhesion enhanced with LePage Ultra Gel super glue). This change created four thermal history treatments during the second year (cool

summer–cool summer, CC; cool–warm, CW; warm–cool, WC; and warm–warm, WW; n = 24).
Sample sizes varied over time due to tile damage and dislodgement (Appendix S1: Fig. S3).

Temperature measurements

For small ectotherms with a large area of attachment to the substratum (e.g., barnacles), substratum temperature is a reasonably good proxy for body temperature (Kordas et al. 2015). Thus, the substratum temperature of both settlement tiles and adjacent bedrock were collected using pre-programmed iButton temperature loggers (model DS1921G-F5# Thermochron, Dallas Semiconductor, USA). To record tile temperature, loggers were sealed in nitrile pouches and sandwiched between the two plates of experimental tile units. To record bedrock temperature, loggers were wrapped in Parafilm and affixed to shore with a 2–3 mm layer of A–788 Splash Zone epoxy (Pettit Paints, USA) separating the logger from both the underlying shore and surrounding air. The number of loggers recording within each treatment varied through time due to changes in the number of treatment groups between years and instrument failure. Temperatures were recorded hourly except over the second winter of the study, when temperatures were instead recorded every two hours.

Community surveys

We characterized organism abundance and community diversity through regular visual surveys of tiles and destructive sampling at the end of the study. Visual surveys occurred approximately monthly during summer and every two months during winter from 8 May 2019 to 24 February 2021. During surveys, each invertebrate species was counted and the percent cover of each algal species was recorded. Organisms were identified to species except for amphipods

and isopods, which were identified to order, and diatom mats, which were lumped into one taxon. Sessile species were only recorded within the central 6.4×6.4 cm area of the epoxy settlement surface using a wire mesh quadrat (mesh size = $6.4 \text{ mm} \times 6.4 \text{ mm}$) to avoid edge effects. Any sessile species growing on the colored tile borders were removed during surveys. Motile invertebrates were counted on the entire tile surface, including on colored tile borders where their influence on the experimental community could not be ruled out. We destructively sampled half of the tiles within each treatment and block on 14 September 2020 (permanently removing these from the study) and sampled remaining tiles on 24 February 2021, scraping all biota from the settlement surface into containers of 70% ethanol (v/v in water). Epifauna were identified and counted under a dissecting microscope. Intertidal organisms were collected under Fisheries and Oceans Canada scientific collection permits (XR 61 2019 and XR 196 2020).

Statistical analyses

We used linear mixed effects models, constructed with *glmmTMB* (Brooks et al. 2017), to test for differences in mean daily maximum (MDM) temperature between treatments. Because of frequent logger failures, temperature records for individual tiles were often incomplete, potentially biasing data. Thus, we imputed missing hourly temperatures with the *mice* package (van Buuren and Groothuis-Oudshoorn 2011) for all bedrock temperature records and the two most complete tile records per year two treatment in each block (i.e, for bedrock, $N=6$ and for tiles $N=12$ in year two, $N=24$ in year one). Data from each year were imputed separately using five iterations with the classification and regression trees method, with hourly ERA5 satellite-derived 2m surface temperature (Hersbach et al. 2023) used as an auxiliary variable. The resulting set of imputations was averaged. Because differences were driven by solar irradiance,

temperature data were retained only if they were collected during daytime summer low tides (1 May – 31 August; see Appendix S1 for details), when treatment differences were likely strongest. Calculated MDM temperatures were modeled as a function of treatment. Random intercept effects of individual tile and date were included, the latter with an AR(1) process to account for autocorrelation.

We tested how temperature treatments affected barnacle recruitment and abundance, grazer abundance, and alpha diversity using generalized linear models with *glmmTMB* (Brooks et al. 2017). Differences in barnacle recruitment between treatments were evaluated during peak recruitment (May or June), while differences in adult abundance were evaluated in winter when spring recruits had reached maturity. Grazer abundance and community diversity were evaluated at the end of summer to characterize the immediate effects of heat stress and again in late winter to allow an opportunity for community recovery. During the first year, responses were modeled as a function of the treatment (cool or warm), while during the second year, they were modeled as a function of the factorial combination of year one treatment and year two treatment. Experimental block was included as a random effect. A fixed effect for original grazer treatments (see details in Appendix S1) was initially included in models of data collected from 8 May 2019 until September 2020, one year after manipulations ceased. If this term was significant, data were not analyzed (true for algal Shannon diversity and cover in year one); if this term was not significant, then it was dropped from the model. Grazer abundance data collected prior to September 2020 were not modeled due to initial grazer community manipulations. Model assumptions were checked using the *DHARMa* package (Hartig 2022). Species richness was log-transformed in for the post-summer timepoint in year two to ensure the model met assumptions. *P*-values were calculated using the Anova function within the *car* package (Fox and Weisberg

2019) with a significance threshold of $P = 0.05$. We also chose to use multiple comparisons tests (Tukey-Kramer *post hoc* tests) to detect differences between treatment combinations because we expected the consistently warm treatment to have substantially different structure than other treatments (Hypothesis 3). For these tests, we used the *emmeans* package (Lenth 2022).

Given the complex and, at times, opposite effects of temperature on algal cover over time, we used generalized additive modeling with the *mgcv* package (Wood 2011) to analyze how temperature affected algal cover dynamics during each year. Within these autoregressive AR(1) models, we included linear terms — for year one, treatment alone, and for year two, an factorial combination of treatments in year one and year two — smooth terms of time (days since the experiment start) for each treatment, and a random effect of block. Pairwise differences in algal cover over time between control treatments (C or CC) and other treatments were calculated and visualized using the methods of Rose et al. (2012). Early grazer manipulations exerted a significant effect on algal cover during the first year, and thus survey data collected during the first year were excluded from analysis.

Treatment-driven differences in epifaunal community structure and beta diversity were modeled with the *vegan* package (Oksanen et al. 2020) for communities immediately following summer heat stress and after winter recovery in the second year of study. Data were ordinated using distance-based redundancy analysis with Bray-Curtis distances. Community structure was modeled as a function of the interaction of treatment in year one and year two using PERMANOVA analyses with 9999 permutations constrained within experimental blocks. Multiple pairwise comparisons were made with *multiconstrained* in the *BiodiversityR* package (Kindt and Coe 2005). Beta diversity was modeled as a function of treatment using PERMDISP analyses with bias adjustment for small sample sizes.

To reflect our underlying analyses, results are subsequently reported by response variable. We relate patterns in each biological response to our initial hypotheses (H1–H3) in Appendix S1: Table S3 and report all the statistical outputs of our models in Appendix S2.

RESULTS

Differences in substratum temperature

Substratum temperatures differed significantly among the cool treatment (white tiles), warm treatment (black tiles), and adjacent bedrock during daytime low tides from May through August. Mean daily maximum (MDM) summer temperatures were consistently ~2 °C higher in warm versus cool treatments (Appendix S1: Table S2), with a grand mean of 29.2 ± 7.0 °C across all warm treatments and 27.1 ± 6.4 °C across all cool treatments. Meanwhile, bedrock was 28.5 ± 7.0 °C during the first summer and 28.1 ± 6.4 °C during the second summer. During the first summer, both the warm treatment and bedrock had significantly higher MDM temperatures than the cool treatment (Figure 2; ANOVA: $\chi^2_2 = 40.53$, $P < 0.001$; Appendix S2: Tables S1–2). During the second summer, warm treatments had significantly higher MDM temperatures than cool treatments, with bedrock temperatures intermediate and statistically similar to all other treatments (ANOVA: $\chi^2_4 = 52.34$, $P < 0.001$; Appendix S2: Tables S3–4). During the second year, taped tile surfaces effectively mimicked the treatment effect of bare tile surfaces (i.e., WC and CW had analogous MDM temperatures to CC and WW, respectively; Appendix S2: Table S7). Mean substratum temperatures displayed analogous patterns to MDM temperatures (Appendix S1: Table S3; Fig. S5; Appendix S2: Tables S5–8).

Effects on barnacle recruitment and abundance

Warm summer temperatures tended to reduce the abundance of barnacle recruits. When peak recruitment was observed during the first year (May and June, respectively, for *B. glandula* and *C. dalli*), temperature treatment did not significantly affect *B. glandula* recruitment (Fig. 3a; Appendix S2: Table S9), but *C. dalli* recruitment was lower within the warm treatment (Fig. 3b; Type II ANOVA, $\chi^2_1 = 4.13$, $P = 0.0422$; Appendix S2: Table S10). Warming had both contemporaneous and carry-over effects on barnacle recruitment during the peak recruitment window of the second year (June for both species). Fewer *Balanus glandula* were present in warm treatments, whether warming occurred during the second summer (Type III ANOVA, treatment_{y2}; $\chi^2_1 = 38.34$, $P < 0.001$; Appendix S2: Tables S11–12) or during the first summer (treatment_{y1}; $\chi^2_1 = 6.07$, $P = 0.0138$). The recruitment of *C. dalli* in year two was similarly negatively affected by warming in both years (Fig. 3b; Type III ANOVA; treatment_{y2}: $\chi^2_1 = 19.16$, $P < 0.001$; treatment_{y1}: $\chi^2_1 = 5.56$, $P = 0.0184$; Appendix S2: Tables S13–14).

Warming reduced the abundance of adult *B. glandula*, but not adult *C. dalli*. At the end of the first winter, there were substantially fewer adult *B. glandula* in the warm treatment (Fig. 3c; Type II ANOVA; $\chi^2_1 = 106.20$, $P < 0.001$; Appendix S2: Table S15). At the end of the study, *B. glandula* abundance appeared to be lower where warming was applied in both summers, but this trend lacked significant statistical support (Type III ANOVA; $P \sim 0.1$ for treatment_{y1} and treatment_{y2}; Appendix S2: Table S16). However, *post hoc* testing suggested that *B. glandula* was more abundant in the consistently cool treatment compared to the consistently warm treatment (Tukey-Kramer; z ratio = 3.08, $P = 0.0111$; Appendix S2: Table S17). During summer in both years, the mortality of *B. glandula* was higher and surviving barnacles were smaller within warm treatments (Appendix S1: Fig. S7–8; Appendix S2: Tables S18–21). The abundance of adult *C. dalli* was similar between treatments in both years (Fig. 3d; Appendix S2: Tables S22–24).

Effects on grazer abundance

During the second year of study, grazer abundance was negatively correlated with warming. Warming had a contemporaneous effect on limpet abundance (Fig. 4a), both immediately following summer (September 2020; Type III ANOVA; $\chi^2_1 = 11.07$, $P < 0.001$; Appendix S2: Tables S25–26) and at the end of winter (February 2021; Type III ANOVA; $\chi^2_1 = 3.87$, $P = 0.0491$; Appendix S2: Tables S26–27). Post-summer littorine snail abundance was lower in warm treatments, whether warming was applied during the first or second summer (Fig. 4b; Type III ANOVA; treatment_{y1} : $\chi^2_1 = 17.56$, $P < 0.001$; treatment_{y2} : $\chi^2_1 = 13.38$, $P < 0.001$; Appendix S2: Tables S28–29). Similar trends in littorine snail abundance were observed at the end of winter, though with reduced statistical support (Type III ANOVA; treatment_{y1} : $\chi^2_1 = 3.29$, $P = 0.0698$; treatment_{y2} : $\chi^2_1 = 3.87$, $P = 0.0491$; Appendix S2: Tables S30–31).

Effects on algal cover

Algal cover and the timing of algal blooms differed between treatments, particularly in the first year of study (Fig. 5a-b). Algal cover reached a similar maximum between treatments, driven by a bloom of the green ephemeral alga *Ulothrix* sp. near the end of the first summer. However, the temporal dynamics of algal cover differed between treatments; cover peaked earlier and declined more rapidly within the cool treatment relative to the warm treatment. After ineffectual grazer manipulations were abandoned during the first year, algal cover in the warm treatment remained significantly higher than in the cool treatment until winter (Fig. 5b; *gamm*; $t = 3.30$, $P = 0.00109$; Appendix S2: Table S32). During the second year, algal cover remained relatively low, but was higher in treatments that alternated thermal conditions relative to those

that were consistently cool or warm (*gamm*; $t = -2.57$, $P = 0.0104$; Appendix S2: Table S33).

Effects on diversity

Warming tended to reduce alpha diversity and alter community structure, particularly in communities that experienced successive warm summers. During the first year, species richness was lower in the warm treatment, whether richness was assessed immediately after summer (Fig. 6a; Type II ANOVA; $\chi^2_1=16.33$, $P < 0.001$; Appendix S2: Table S34) or at the end of winter (Type II ANOVA; $\chi^2_1=74.85$, $P < 0.001$; Appendix S2: Table S35). During the second year, post-summer species richness was lower in treatments that experienced contemporaneous warming (Fig. 6b; Type III ANOVA; $\chi^2_1=4.73$, $P = 0.0297$; Appendix S2: Tables S36–37), but were unaffected by warming applied in the first year. After winter recovery, no overall effect of temperature treatment in either summer was discernible (Appendix S2: Table S38), but *post hoc* pairwise comparisons suggested that the treatment that was successively warmed had lower diversity than treatments that were cool during the second summer (Appendix S2: Table S39; Tukey-Kramer; CC–WW: z ratio = 3.87, $P < 0.0001$; WC–WW: z ratio = 3.27, $P = 0.00590$). Warming also exerted a negative effect on the Shannon diversity of the invertebrate community; during winter of the first year, diversity was significantly lower within the warm treatment, and during the second year, diversity was lower in treatments where warming was applied during the first year (Appendix S1: Fig. S11a–b, Appendix S2: Tables S40–45). The Shannon diversity of the algal community, meanwhile, was reduced by warm temperatures during the first year, but not affected during the second year (Appendix S1: Fig. S11c, Appendix S2: Tables S46–48).

Epifaunal communities characterized on destructively sampled tiles demonstrated that community structure, but not beta diversity, differed between treatments. At the end of the

second summer (September 2020; Fig. 6c), there were no significant differences in community structure between treatments based on PERMANOVA (Appendix S2: Table S49), though *post hoc* pairwise comparisons indicated the CC and WW treatments differed in composition (Appendix S2: Table S50; *multiconstrained*; $F_1 = 2.68$, $P = 0.018$). At the end of the experiment (February 2021; Fig. 6d), however, warm temperatures in year one and year two interacted to drive differences in community structure (PERMANOVA; $F_{1,37} = 2.22$, $P = 0.0125$; Appendix S2: Table S51). *Post hoc* comparisons showed that this was primarily driven by differences between the structure of the consistently cool treatment and all others (Appendix S2: Table S52). Beta diversity was similar among treatments (Appendix S2: Tables S53–54). The alpha diversity of these epifaunal communities was generally lowest in the consistently warm treatment, particularly compared with samples where temperatures were cool during the second summer (Appendix S1: Figure S12; Appendix S2: Tables S55–62).

DISCUSSION

In this study, we passively manipulated the substratum temperature of intertidal settlement tiles over two consecutive summers to determine the effects of present and past warming and whether prior thermal stress influences the impact of subsequent thermal stress. We expected that warming would have contemporaneous direct negative effects on organism abundance and diversity (H1) and persistent indirect negative effects mediated by lower foundation species cover (H2). We expected that warming during the second year would have greater negative effects where conditions were previously warm, since foundation species cover and thus thermal refugia would be constrained, thereby increasing stress for associated biota (H3). As anticipated, we found that warming often had both contemporaneous and persistent

negative effects on organism abundance and community alpha diversity, though its effects on algae were more complex. Contrary to our prediction, the magnitude of the effects of warming in the second summer were usually independent of whether warming had been previously applied.

The methodology employed in this study was effective in manipulating substratum temperatures. In both years, the surfaces of white tiles were cooler than those of black tiles, as in previous studies (Kordas et al. 2015, 2017). Interestingly, bedrock temperatures were more analogous to those of black tiles during the first year. This unexpected pattern could be an artefact of shading from copper fences that encircled tiles for most of the first summer, but not the second, which may have artificially cooled tile surfaces relative to adjacent bedrock. The intermediate temperatures of bedrock recorded in the second year of study may reflect its grey color, which absorbs more solar insolation than a purely white surface, but reflects more solar insolation than a purely black surface. Regardless of trends in bedrock temperature, the temperatures of white (cool) and black (warm) tiles and the degree of difference between them were consistent across years, which drove corresponding biological differences.

The recruitment and abundance of acorn barnacle foundation species (*B. glandula* and *C. dalli*) was typically lower within warm treatments, consistent with past studies (Kordas et al. 2015, 2017, Kordas and Harley 2016). For *B. glandula*, the dominant barnacle in this system, the highest recorded LT₅₀ in air is 43 °C (Hamilton and Gosselin 2020), though mortality has been observed at 40 °C (Ober et al. 2019). Substratum temperatures within all treatments exceeded these lethal thresholds during daytime summer low tides, with warm treatments reaching 45 °C during both years. While barnacles tend to remain slightly cooler than surrounding bedrock (Harley and Lopez 2003), the higher mortality we observed for *B. glandula* within warm treatments suggest that barnacle body temperatures, particularly on black tiles, exceeded critical

thermal limits. Even exposure to sublethal temperatures can incur metabolic costs; high temperatures can impair *B. glandula* respiration for many hours after exposure (Ober et al. 2019), and sustained warm temperatures can slow barnacle growth (Kordas and Harley 2016). Here, *B. glandula* tended to be smaller within warm treatments, indicating that surviving barnacles experienced sublethal thermal stress that impaired growth. The tendency of barnacles to settle gregariously may magnify direct negative effects on abundance and recruitment if warming is sustained. Barnacles preferentially recruit to areas containing conspecifics, a strategy that increases the likelihood of successful sexual reproduction via internal fertilization (Wu 1981). Thus, recruitment to previously warm tiles during the second year may have been lower because these tiles hosted fewer adult barnacles. The other acorn barnacle present, *C. dalli*, was not prevalent during the first year, possibly due to interannual variation in recruitment dynamics common in barnacles (Scrosati and Ellrich 2016). Recruitment in the second year was lower within warm treatments, but adult abundance was unaffected by treatment, possibly because adult *C. dalli* are more robust to thermal stress than *B. glandula*, with an LT_{50} near 44.5 °C (Hamilton and Gosselin 2020). Grazer manipulations during the first summer may have reduced barnacle recruitment and hampered the detection of a treatment effect, since limpets, which were purposefully included or excluded from both white and black tiles, are known to remove barnacle recruits during grazing (Dayton 1971).

During the second year, reduced grazer abundance in the warm treatments may have been due to the direct effects of temperature and/or indirect effects mediated by differences in barnacle abundance. One common limpet in this system, *Lottia digitalis*, has an upper thermal limit of 38 °C in air (Bjelde and Todgham 2013). High intertidal littorine snails have a slightly greater tolerance to elevated temperatures (41.01 °C for *L. sitkana* and 41.47 °C for *L. scutulata*

during five-hour emersions; Stickle et al. 2017). While these dominant grazers are thermally robust, recorded summer substratum temperatures frequently exceeded these thresholds for short periods. Temperatures likely regularly fluctuated above grazer thermal optima (e.g., 30 °C for *L. digitalis*; Bjelde and Todgham 2013), which could have suppressed grazer activity, and thus foraging effectiveness (Rickards and Boulding 2015). Motile organisms can behaviourally thermoregulate by moving to avoid thermal stress. Grazers were not commonly observed on tiles during the summer, though surveys occurred exclusively at low tide, when some grazers avoid feeding (Little 1989), and we may have thus underestimated abundance. However, these temporal dynamics suggest that, while warm temperatures may have directly reduced grazer abundance, indirect effects are more likely. Limpets and littorine snails were generally more abundant within cool treatments where barnacle cover was higher, a pattern consistent with other studies (Silva et al. 2015, Hesketh et al. 2021). Barnacles can reduce desiccation stress for associated species by creating moist, humid microhabitats during low tides (Vermeij 1978; Harley and O'Riley 2011); thus, the abundant, larger barnacles present on cool tiles may have generated a higher density of favorable microhabitats, begetting a higher abundance of grazers.

Barnacles, in addition to providing microhabitats, may have influenced grazer abundance through their effects on algal food supply. The green filamentous *Ulothrix* sp. initially dominated bare tiles, but eventually declined and was replaced by other foliose algal species — usually growing on barnacle tests — a pattern observed in past studies (Kordas et al. 2017). While maximum algal cover was similar between temperature treatments during the first year, its temporal dynamics differed; algal cover peaked later and declined more slowly within the warm treatment. High temperatures can have highly variable interspecific effects on algae (Kordas et al., 2017). *Ulothrix* sp. may have thrived under warm summer conditions due to higher growth

rates, because grazer activity was suppressed by high temperatures, or because barnacles, which can compete with algae for space or harbor populations of voracious grazers (Hesketh et al. 2021), were less abundant and smaller. On adjacent bedrock, *Ulothrix* sp. was most commonly observed in bare, log-damaged patches within barnacle beds, supporting an indirect negative effect of barnacles on this species (as has been documented with the ephemeral green alga *Urospora* spp.; Harley 2006). Meanwhile, other algae (here, *Pyropia* sp. and *Ulva* sp.) may preferentially attach to rugose barnacle tests, and barnacles can provide refuge from desiccation and grazing (particularly by limpets) for algal spores and germlings (Farrell 1991; Geller 1991). Thus, algal cover may have been highest in the warm-cool and cool–warm treatments during the second year because shifting thermal conditions created a heterogeneous mixture of bare space and sparse barnacles, allowing for the growth of both desiccation-tolerant, barnacle-phobic and desiccation-intolerant, barnacle-philic algae.

Thermal stress, by shaping barnacle, grazer, and algal populations, had higher-level impacts on diversity and community structure. Alpha diversity generally increased over the course of succession but remained lower in warm treatments, as has been found previously (Kordas et al. 2015, Kordas et al. 2017). Barnacle recruits, followed by opportunistic ephemeral algae, appeared shortly after tiles were installed, consistent with studies involving intertidal disturbance and succession in the northeast Pacific (Farrell 1991, Geller 1991). Because barnacles act as both facilitators (Farrell 1991) and food sources (Harley and O’Riley 2011) within the high intertidal zone, their presence allowed grazers (e.g., amphipods, limpets), secondary successional species (e.g., perennial algae), and predators (e.g., ribbon worms) to enter the nascent community. Of all treatments, the consistently cool and consistently warm treatments were most different in their composition, indicating that persistent thermal stress

shapes not only the diversity of, but also the identity of, species within communities. Thus, the higher alpha diversity and differing community structure of cool compared to warm treatments may have been driven by the facilitatory ability of larger, more abundant barnacles, by more and/or different species surviving under thermally benign versus thermally taxing conditions, or — more likely — by a mixture of these two mechanisms. Disentangling these indirect and direct effects is challenging given the experimental design employed.

Because foundation species (barnacle) cover was lower within the warm treatment compared to the cool treatment after the first year, we anticipated that the effects of warm temperatures would be magnified during the second year. However, the negative effect of warming in the second summer was independent of warming in the first year. While intertidal foundation species can improve the survival, growth, and diversity of associated species in the face of thermal stress (Jurgens et al. 2022; Hesketh and Harley 2023), the size and density of foundation species can affect their facilitative ability (Irving and Bertness 2009). Here, though *B. glandula* had generally surpassed the size threshold for sexual maturity (~5 mm; Hines 1976), they may still have been too small or sparse to effectively buffer thermal and desiccation stress (Rickards and Boulding 2015) at the start of the second summer.

While intertidal systems are resilient up to a point, repeated atmospheric warming threatens to disrupt even these historically stalwart communities (Menge et al. 2022). Our results suggest that even for high-turnover barnacle bed communities (Farrell 1991), thermal stress exerts lasting effects on community structure by reducing barnacle density. Increasing mean temperatures and intensifying heatwaves may cause substantial mortality (Hesketh and Harley 2023) and accelerate shifts in ecological communities (Harris et al. 2018). Climate change also encompasses multiple stressors beyond temperature that may co-occur and interact with warming

(MacLennan and Vinebrooke 2021). To understand the full risk of climate change to ecological communities, we must embrace complexity by integrating stochasticity, considering the temporal dimensions of stress, and seeking to emulate natural processes within our experimental designs.

CONFLICT OF INTEREST: The authors declare no conflicts of interest.

ACKNOWLEDGEMENTS: We thank the Coast Salish peoples on whose traditional, sovereign, and unceded territory this work was conducted. We thank S. Blain, A. Holland, and G. Brownlee for field work assistance, B. Gillespie and V. Grant for help constructing tiles, and BC Parks for site access. Thanks to R. Germain, C. Brauner, S. Dudas and two anonymous reviewers for their feedback on this work. National Geographic provided funding through AVH (EC-54154R-18). Additional support was provided to CDGH through Canadian Healthy Oceans Network (NETGP 468437-14) and an NSERC Discovery Grant (RGPIN-2016-05441).

REFERENCES

- Barnes, M. 2000. The use of intertidal barnacle shells. In: *Oceanography and Marine Biology: an Annual Review*. Taylor & Francis, pp. 157–187.
- Bates, D., Mächler, M., Bolker, B. and Walker, S. 2015. Fitting linear mixed-effects models using lme4. *Journal of Statistical Software* 67: 1–48.
- Bjelde, B. E. and Todgham, A. E. 2013. Thermal physiology of the fingered limpet *Lottia digitalis* under emersion and immersion. *Journal of Experimental Biology* 216: 2858–2869.
- Brooks, M.E., Kristensen, K., van Benthem, K.J., Magnusson, A., Berg, C.W., Nielsen, A., Skaug, H.J., Maechler, M. and Bolker, B.M. 2017. glmmTMB balances speed and flexibility

among packages for zero-inflated generalized linear mixed modeling. *The R Journal* 9: 378400

Bulleri, F., Bruno, J. F., Silliman, B. R. and Stachowicz, J. J. 2016. Facilitation and the niche: implications for coexistence, range shifts and ecosystem functioning. *Functional Ecology* 30: 70–78.

Dal Bello, M., Rindi, L. and Benedetti-Cecchi, L. 2019. Temporal clustering of extreme climate events drives a regime shift in rocky intertidal biofilms. *Ecology* 100: e02578.

Dayton, P. K. 1971. Competition, disturbance, and community organization: The provision and subsequent utilization of space in a rocky intertidal community. *Ecological Monographs* 41: 351–389.

Farrell, T. M. 1991. Models and mechanisms of succession: An example from a rocky intertidal community. *Ecological Monographs* 61: 95–113.

Fox, J. and Weisberg, S. 2019. An {R} companion to applied regression, third edition. Thousand Oaks CA: Sage.

Geller, J. B. 1991. Gastropod grazers and algal colonization on a rocky shore in northern California: the importance of the body size of grazers. *Journal of Experimental Marine Biology and Ecology* 150: 1–17.

Gutiérrez, J. L., Bagur, M., Lorenzo, R. A. and Palomo, M. G. 2023. A facultative mutualism between habitat-forming species enhances the resistance of rocky shore communities to heat waves. – *Frontiers in Ecology and Evolution* 11: 1278762.

Hamilton, H. and Gosselin, L. 2020. Ontogenetic shifts and interspecies variation in tolerance to desiccation and heat at the early benthic phase of six intertidal invertebrates. *Marine Ecology Progress Series* 634: 15–28.

Hammill, E. and Dart, R. 2022. Contributions of mean temperature and temperature variation to

507 population stability and community diversity. *Ecology and Evolution* 12: e8665.

508 Harley, C. D. G. and Lopez, J. P. 2003. The natural history, physiology, and ecological impacts
509 of the intertidal mesopredators, *Oedoparena* spp. (Diptera, Dryomyzidae). *Invertebrate Biology*
510 122:61-73

511 Harley, C. D. G. 2006. Effects of physical ecosystem engineering and herbivory on intertidal
512 community structure. *Marine Ecology Progress Series* 317: 29–39.

513 Harley, C. 2008. Tidal dynamics, topographic orientation, and temperature-mediated mass
514 mortalities on rocky shores. *Marine Ecology Progress Series* 371: 37–46.

515 Harley, C. D. G. and O’Riley, J. L. 2011. Non-linear density-dependent effects of an intertidal
516 ecosystem engineer. *Oecologia* 166: 531–541.

517 Harris, R. M. B., Beaumont, L. J., Vance, T. R., Tozer, C. R., Remenyi, T. A., Perkins-
518 Kirkpatrick, S. E., Mitchell, P. J. et al. 2018. Biological responses to the press and pulse of
519 climate trends and extreme events. *Nature Climate Change* 8: 579–587.

520 Hartig, F. 2021. DHARMA: Residual diagnostics for hierarchical (multi-level/mixed) regression
521 models. R package version 0.4.6.

522 Helmuth, B., Broitman, B. R., Blanchette, C. A., Gilman, S., Halpin, P., Harley, C. D. G.,
523 O’Donnell, M. J., Hofmann, G. E., Menge, B. and Strickland, D. 2006. Mosaic patterns of
524 thermal stress in the rocky intertidal zone: Implications for climate change. *Ecological*
525 *Monographs* 76: 461–479.

526 Hersbach, H., Bell, B., Berrisford, P., Biavati, G., Horányi, A., Muñoz Sabater, J., Nicolas, J. et
527 al. 2023. ERA5 hourly data on single levels from 1940 to present. Copernicus Climate Change
528 Service (C3S) Climate Data Store (CDS). Accessed on 27 December 2024.

529 Hesketh, A. 2024. avhesketh/SVSWS: First release (v1.0.1). Zenodo.

530 <https://doi.org/10.5281/zenodo.15054111>.

531 Hesketh, A. 2024. The effect of single versus successive warm summers on an intertidal
532 community [Dataset]. Zenodo. <https://doi.org/10.5281/zenodo.15054128>.

533 Hesketh, A. V. and Harley, C. D. G. 2023. Extreme heatwave drives topography-dependent
534 patterns of mortality in a bed-forming intertidal barnacle, with implications for associated
535 community structure. *Global Change Biology* 29: 165–178.

536 Hesketh, A. V., Schwindt, E. and Harley, C. D. G. 2021. Ecological and environmental context
537 shape the differential effects of a facilitator in its native and invaded ranges. *Ecology* 102:
538 e03478.

539 Hines, A. H. 1976. Reproduction in three species of intertidal barnacles from Central California.
540 *Biological Bulletin* 154: 262–281.

541 Hughes, T. P., Kerry, J. T., Connolly, S. R., Baird, A. H., Eakin, C. M., Heron, S. F., Hoey, A. S.
542 et al. 2019. Ecological memory modifies the cumulative impact of recurrent climate extremes.
543 *Nature Climate Change* 9: 40–43.

544 IPCC. 2023. Climate Change 2023: Synthesis Report. Contribution of Working Groups I, II and
545 III to the Sixth Assessment Report of the Intergovernmental Panel on Climate Change (Core
546 Writing Team, Lee, H. and Romero, J., Eds.) IPCC, Geneva, Switzerland, pp. 35–115.

547 Irving, A. D. and Bertness, M. D. 2009. Trait-dependent modification of facilitation on cobble
548 beaches. *Ecology* 90: 3042–3050.

549 Jurgens, L. J., Ashlock, L. W. and Gaylord, B. 2022. Facilitation alters climate change risk on
550 rocky shores. *Ecology* 103: e03596.

551 Kindt, R. and Coe, R. 2005. Tree diversity analysis. A manual and software for common
552 statistical methods for ecological and biodiversity studies. Nairobi: World Agroforestry Centre

553 (ICRAF).

554 Kordas, R. and Harley, C. 2016. Demographic responses of coexisting species to *in situ*

555 warming. Marine Ecology Progress Series 546: 147–161.

556 Kordas, R. L., Dudgeon, S., Storey, S. and Harley, C. D. G. 2015. Intertidal community

557 responses to field-based experimental warming. Oikos 124: 888–898.

558 Kordas, R. L., Donohue, I. and Harley, C. D. G. 2017. Herbivory enables marine communities to

559 resist warming. Science Advances 3: e1701349.

560 Lee, R. H., Morgan, B., Liu, C., Fellowes, J. R. and Guénard, B. 2021. Secondary forest

561 succession buffers extreme temperature impacts on subtropical Asian ants. Ecological

562 Monographs 91: e01480.

563 Lenth, R. 2023. emmeans: Estimated marginal means, aka least-squares means. R package

564 version 1.8.6.

565 Little, C. 1989. Factors governing patterns of foraging activity in littoral marine herbivorous

566 molluscs. Journal of Molluscan Studies 55: 273–284.

567 Little, C., Trowbridge, C. D., Williams, G. A., Hui, T. Y., Pilling, G. M., Morritt, D. and Stirling,

568 P. 2021. Response of intertidal barnacles to air temperature: Long-term monitoring and *in-situ*

569 measurements. Estuarine, Coastal and Shelf Science 256: 107367.

570 Ma, C.-S., Wang, L., Zhang, W. and Rudolf, V. H. W. 2018. Resolving biological impacts of

571 multiple heat waves: interaction of hot and recovery days. Oikos 127: 622–633.

572 MacLennan, M. M. and Vinebrooke, R. D. 2021. Exposure order effects of consecutive stressors

573 on communities: The role of co-tolerance. Oikos 130: 2111–2121.

574 Menge, B. A., Gravem, S. A., Johnson, A., Robinson, J. W. and Poirson, B. N. 2022. Increasing

575 instability of a rocky intertidal meta-ecosystem. Proceedings of the National Academy of

576 Sciences U.S.A. 119: e2114257119.
 577 Montie, S. and Thomsen, M. S. 2023. Long-term community shifts driven by local extinction of
 578 an iconic foundation species following an extreme marine heatwave. Ecology and Evolution
 579 13: e10235.
 580 Ober, G., Rognstad, R. and Gilman, S. 2019. The cost of emersion for the barnacle *Balanus*
 581 *glandula*. Marine Ecology Progress Series 627: 95–107.
 582 Oliver, E. C. J., Donat, M. G., Burrows, M. T., Moore, P. J., Smale, D. A., Alexander, L. V.,
 583 Benthuisen, J. A. et al. 2018. Longer and more frequent marine heatwaves over the past
 584 century. Nature Communications 9: 1324.
 585 Oksanen, J., Blanchet, F.G., Friendly, M., Kindt, R., Legendre, P., McGlinn, D., Minchin, P.R. et
 586 al. 2020. vegan: Community Ecology Package. R package version 2.6-4.
 587 Pansch, C., Scotti, M., Barboza, F. R., Al-Janabi, B., Brakel, J., Briski, E., Buscholz, B. et al.
 588 2018. Heat waves and their significance for a temperate benthic community: A near-natural
 589 experimental approach. Global Change Biology 24: 4357–4367.
 590 Perkins-Kirkpatrick, S. E. and Lewis, S. C. 2020. Increasing trends in regional heatwaves.
 591 Nature Communications 11: 3357.
 592 Rickards, K. and Boulding, E. 2015. Effects of temperature and humidity on activity and
 593 microhabitat selection by *Littorina subrotundata*. Marine Ecology Progress Series 537: 163–
 594 173.
 595 Rose, N. L., Yang, H., Turner, S. D. and Simpson, G. L. 2012. An assessment of the mechanisms
 596 for the transfer of lead and mercury from atmospherically contaminated organic soils to lake
 597 sediments with particular reference to Scotland, UK. Geochimica et Cosmochimica Acta 82:
 598 113–135.

599 Scrosati, R. A. and Ellrich, J. A. 2016. A 12-year record of intertidal barnacle recruitment in
 600 Atlantic Canada (2005–2016): Relationships with sea surface temperature and phytoplankton
 601 abundance. *PeerJ* 4: e2623–e2623.

602 Siegle, M. R., Taylor, E. B. and O’Connor, M. I. 2022. Heat wave intensity drives sublethal
 603 reproductive costs in a tidepool copepod. *Integrative Organismal Biology* 4: obac005.

604 Silva, A. C. F., Mendonça, V., Paquete, R., Barreiras, N. and Vinagre, C. 2015. Habitat provision
 605 of barnacle tests for overcrowded periwinkles. *Marine Ecology* 36: 530–540.

606 Stickle, W. B., Carrington, E. and Hayford, H. 2017. Seasonal changes in the thermal regime and
 607 gastropod tolerance to temperature and desiccation stress in the rocky intertidal zone. *Journal of*
 608 *Experimental Marine Biology and Ecology* 488: 83–91.

609 van Buuren, S., Groothuis-Oudshoorn K. 2011. mice: Multivariate Imputation by Chained
 610 Equations in R. *Journal of Statistical Software*, 45: 1-67.

611 Vasseur, D. A., DeLong, J. P., Gilbert, B., Greig, H. S., Harley, C. D. G., McCann, K. S.,
 612 Savage, V., Tunney, T. D. and O’Connor, M. I. 2014. Increased temperature variation poses a
 613 greater risk to species than climate warming. *Proceedings of the Royal Society B*. 281:
 614 20132612.

615 Vermeij, G. J. 1978. *Biogeography and Adaptation: Patterns of Marine Life*. Harvard University
 616 Press.

617 Wood, S. N. 2011. Fast stable restricted maximum likelihood and marginal likelihood estimation
 618 of semiparametric generalized linear models. *Journal of the Royal Statistical Society (B)* 73: 3–
 619 36.

620 Wu, R. S.-S. 1981. The effect of aggregation on breeding in the barnacle *Balanus glandula*,
 621 Darwin. *Canadian Journal of Zoology* 59: 890–892.

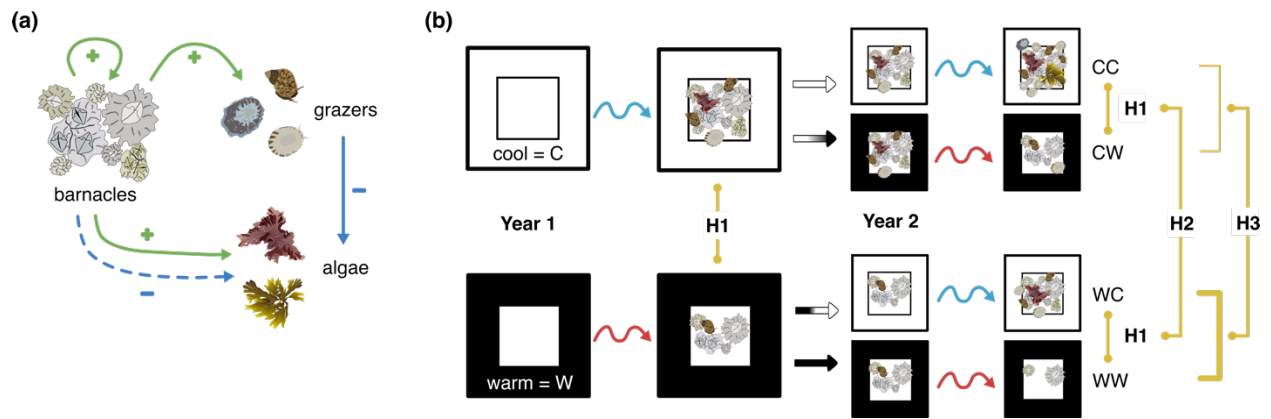


Figure 1

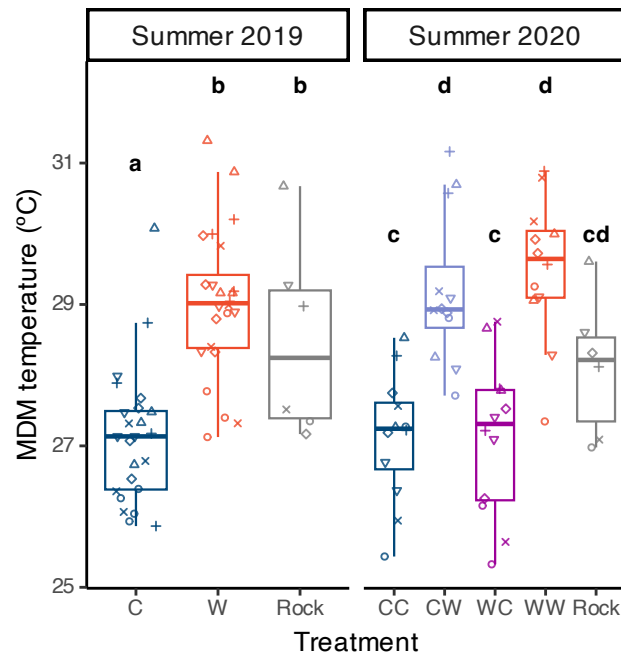


Figure 2

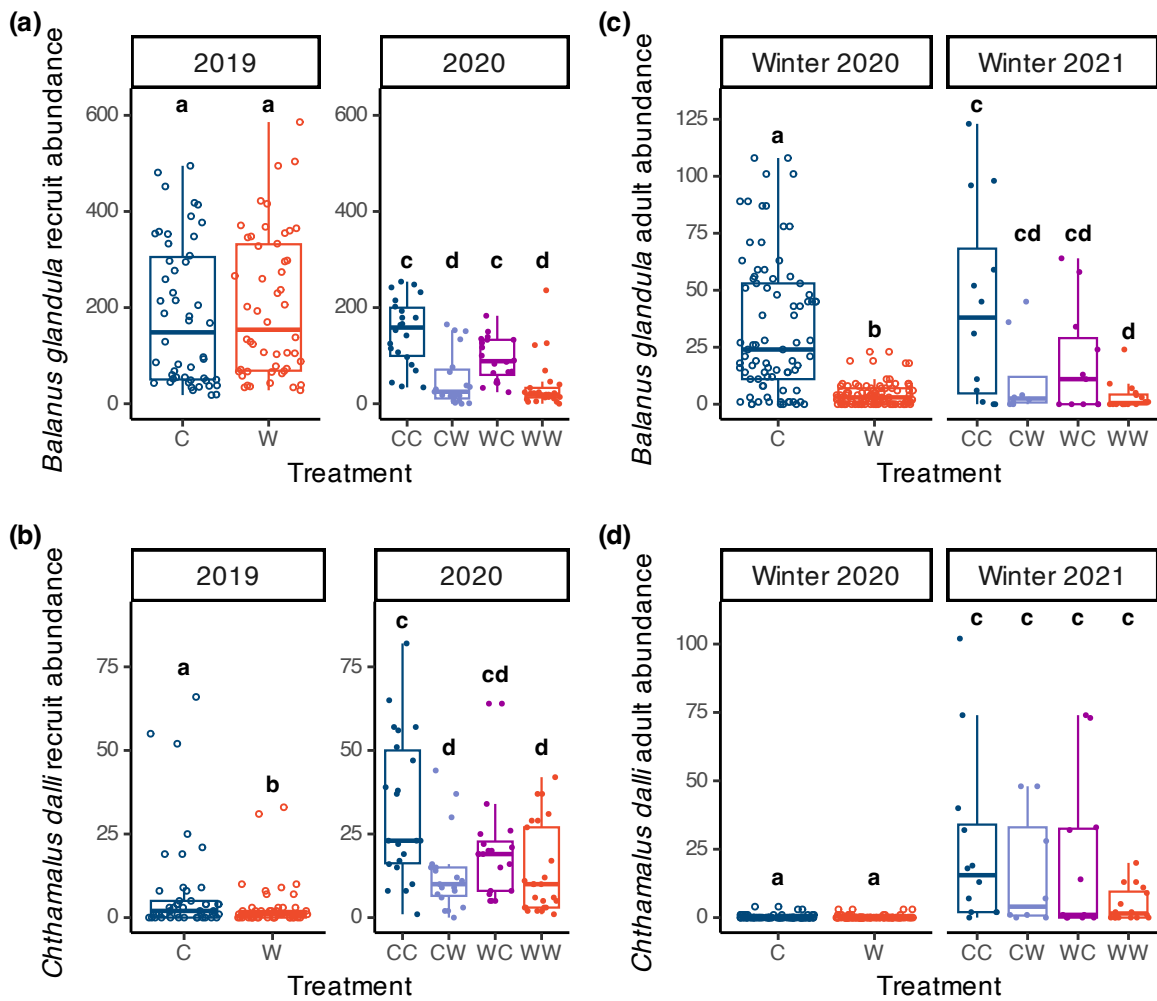


Figure 3

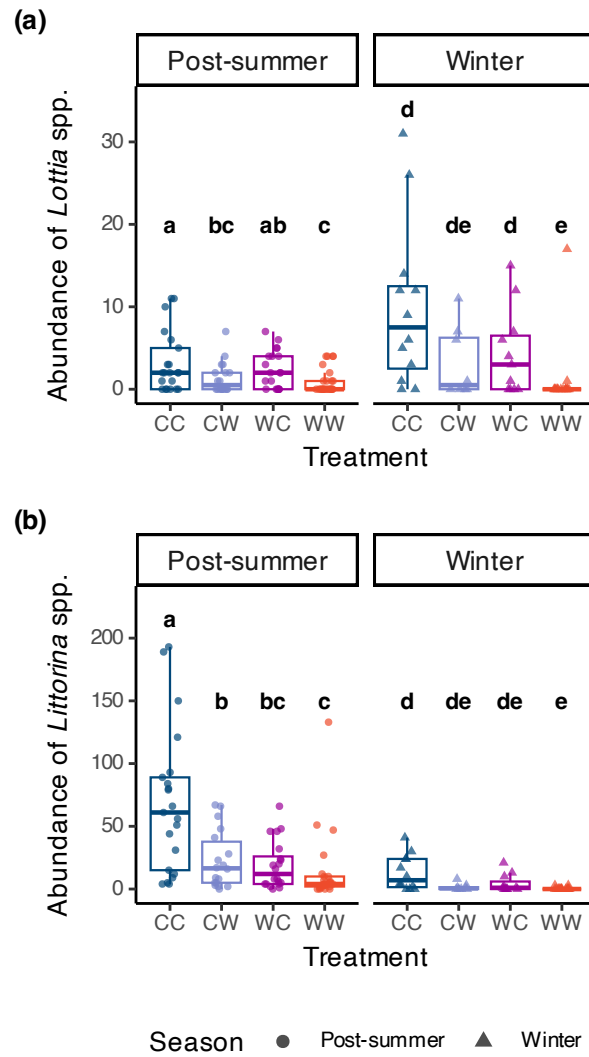
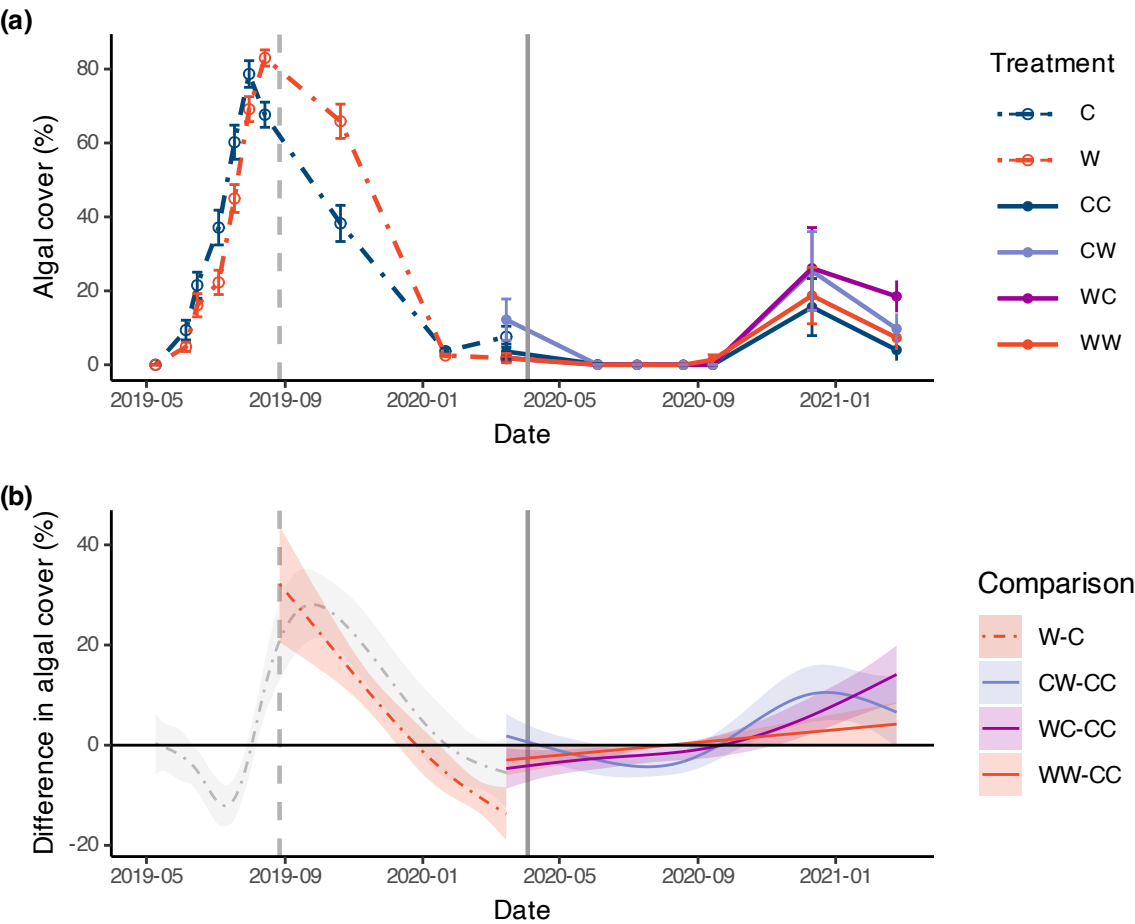


Figure 4

655



656

657

Figure 5

658

659

660

661

662

663

664

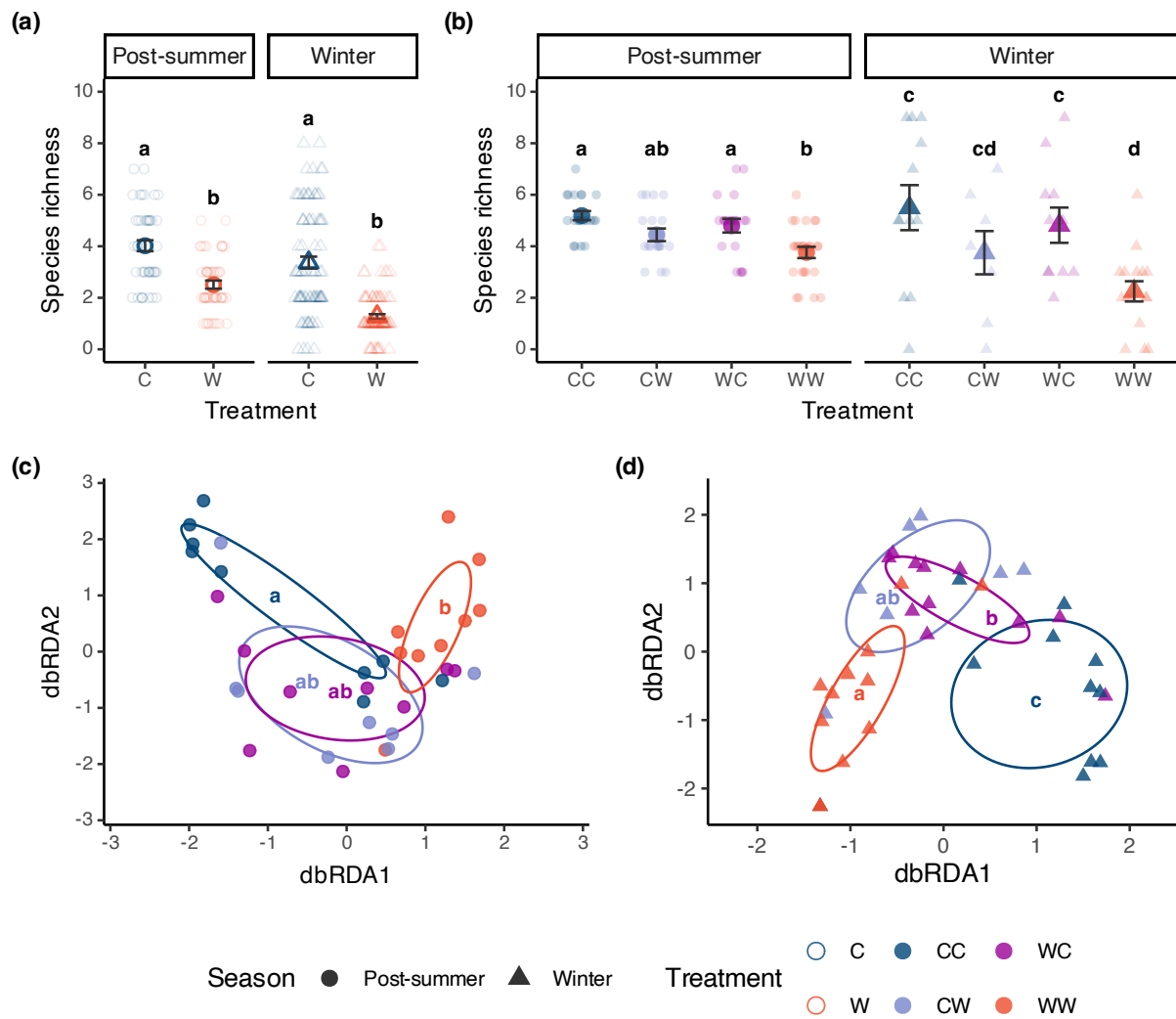


Figure 6

Figure 1. (a) Simplified interaction diagram for a *Balanus glandula*-dominated intertidal community in the northeast Pacific. Barnacles facilitate gregarious barnacle recruitment and the presence of grazers and algae through habitat provision and moisture retention, while grazers consume algae. **(b)** Experimental design for this multi-year warming study and treatment comparisons to address hypotheses (H1–H3). White (cool = C) tiles and black (warm = W) settlement tiles were installed in the intertidal zone before the onset of summer. Tiles were then exposed to summertime low tides, wherein warming was expected to drive temperature-linked differences in community composition. At the start of the second year, the colour of half of each treatment was swapped using heavy-duty tape, generating four treatments (CC, CW, WC, and WW) that were monitored until the end of Year 2. Digital art by Amelia V. Hesketh.

Figure 2. Differences in residual mean daily maximum substratum temperatures of experimental tiles and adjacent bedrock recorded by temperature loggers at TESNO, EN. Points represent the mean value for each experimental tile for which temperature was measured, with different shapes used to represent each experimental block (n=4 per treatment per block in year one, n=2 per treatment per block in year two, n=1 per block for rock temperature in both years). Only temperature data collected during daytime summer low tides between 1 June – 31 August were used. Bold lowercase letters represent statistically different groups, as determined by Tukey-Kramer *post hoc* tests on temperature models. C = cool summer, W = warm summer, CC = cool–cool, CW = cool–warm, WC = warm–cool, WW = warm–warm.

Figure 3. Temperature-driven differences in acorn barnacle abundance on experimental tiles at TESNO, EN, in terms of **(a)** abundance of *B. glandula* and **(b)** *C. dalli* recruits during peak

observed recruitment (*B. glandula* May 2019: n = 50; *C. dalli* June 2019: n = 46 and 50 for C and W, respectively; 4 June 2020: n = 22, 19, 20, and 25 for CC, CW, WC, and WW) and (c) abundance of *B. glandula* and (d) *C. dalli* adults at the end of the first and second winters (March 2020: n=82 for C, n=91 for W; February 2021: n = 12, 8, 11, and 16 for CC, CW, WC, and WW). Letters indicate significant differences between treatment groups determined by Type II ANOVA (year one) and Tukey-Kramer *post hoc* tests (year two). Treatment codes as in Fig. 1.

Figure 4. Temperature-driven differences in (a) *Lottia* spp. (limpet) and (b) *Littorina* spp. (littorine snail) abundance on experimental tiles at TESNO, EN immediately following summer (September 2020; n = 21, 18, 20, and 25 for CC, CW, WC, and WW) and during winter (February 2021; n = 12, 8, 11, and 16 for CC, CW, WC, and WW). Grazers were counted on the entire 15 x 15 cm upper surface of the tiles. Bold lowercase letters indicate significant differences between treatment groups determined by Tukey-Kramer *post hoc* tests. See Fig. 1 for treatment codes.

Figure 5. (a) Temperature-driven differences in algal cover on experimental tiles at TESNO, EN. (b) Pairwise differences in fitted *gamm* smoothers for algal cover in the control (C or CC) treatment and all other treatments. Shaded areas represent an approximate 95% pointwise confidence interval; when this area does not overlap zero, a significant difference can be inferred. The vertical dashed line indicates when early herbivore manipulations stopped, while the vertical solid line indicates when treatments were swapped at the beginning of year two. During year one, the grey smoother represents *gamm* smoother differences (W-C comparison) when all data are modeled; the red smoother represents *gamm* smoother differences with data

removed for the period that grazer manipulations were active.

Figure 6. Temperature-driven differences in intertidal community diversity on experimental tiles at TESNO, EN. **(a)** Species richness in year one and **(b)** in year two, determined from visual surveys post-summer and during late winter. Error bars represent standard error about the mean. Symbols/letters denote differences between treatment groups determined by Type II ANOVA (year one) and Tukey-Kramer *post hoc* tests (year two). **(c)** Community structure of destructively sampled epifauna in September 2020 and **(d)** February 2021, plotted in multidimensional space using distance-based redundancy analysis with Bray-Curtis distances. Each point represents a single experimental tile. In year one, n = 47 and 49 for C and W, respectively post-summer and n = 41 and 46 for C and W, respectively, in winter. For year two, n = 21, 18, 20, and 25 for CC, CW, WC, and WW post-summer and n = 12, 8, 11, and 16 for CC, CW, WC, and WW during winter. Letters denote differences between treatment groups determined using post-hoc testing through *multiconstrained*.

Studies of organismal responses to ocean change are often conducted within a carefully controlled laboratory setting where the confounding variables present in nature can be more easily removed. Such precision and control, though ideal for uncovering the mechanisms underlying biological responses (e.g., Gimenez et al., 2019), inevitably oversimplify the natural settings in which organisms will encounter environmental drivers and may thus be less realistic and generalizable (De Boeck et al., 2015). In coastal waters, environmental conditions are particularly dynamic. The temperature and salinity of coastal surface waters are more spatially and temporally variable than waters further offshore (Ozer et al., 2022). Seawater pH can fluctuate due to seasonal upwelling and downwelling (Fairchild & Hales, 2021; Feely et al., 2008), riverine inputs (Fassbender et al., 2016; Moore-Maley et al., 2018), wind-driven mixing (Moore-Maley et al., 2016), and daily cycles of respiration and photosynthesis by nearshore biota (Ragazzola et al., 2021; Ricart et al., 2021; Wolfe et al., 2020). Abiotic variability can drive fluctuations in the abundance and diversity of plankton communities (e.g., plankton blooms; Bode et al., 2005; Suchy et al., 2019), which can in turn further affect ocean chemistry (Ianson et al., 2016). Within the intertidal zone, conditions are even more variable as marine organisms are periodically exposed to terrestrial conditions such as extremely high and low temperatures (e.g., Harley 2008; Stickle et al., 2015). The use of natural variability through space-for-time field experiments may thus provide a more nuanced and accurate picture of how organisms will respond to ocean change (Cui et al., 2021; Foo & Byrne, 2021; Tito et al., 2020).

Coastal waters, in addition to being highly variable, are often also areas of intensive aquaculture. The Pacific oyster, *Magallana* (= *Crassostrea*) *gigas* (Thunberg 1793), has been introduced as an aquaculture species to temperate coastal waters worldwide, with 0.64 million tonnes being produced globally in 2018 (FAO, 2020). Husbandry practices vary geographically

APPENDIX S2: STATISTICAL OUTPUTS

The effect of single versus successive warm summers on an intertidal community

Amelia V. Hesketh, Cassandra A. Konecny, Sandra M. Emry, Christopher D. G. Harley

Ecology

Analysis 1: Substratum temperature

Model S1

Mean daily maximum temperature \sim treatment + (1 | tile) + (1 | date) + ar1(date - 1 | tile)

Error distribution: Gaussian

Table S1. Model summary table for Model S1, an autoregressive linear mixed effects model testing the effect of treatment on mean daily maximum temperature recorded by temperature loggers during daytime summer low tides of the first year of the thermal manipulation. Random intercept effects were included for individual tile and sampling date, with an autoregressive order 1 process for sampling date to reduce temporal autocorrelation. Coefficients given are relative to the cool treatment, and the model was tested using a Type II ANOVA. SE = standard error, df = degrees freedom.

Term	Coefficient	SE	χ^2	df	P
Intercept	27.038	0.634			
Treatment–Rock	1.410	0.477	40.53	2	1.59x10 ⁻⁹
Treatment–Warm	1.896	0.302			

Table S2. Tukey-Kramer *post hoc* comparison of the mean daily maximum temperatures within treatment groups in year one of the thermal manipulation. SE = standard error, C = cool treatment, W = warm treatment

Contrast	Estimate	SE	df	t ratio	P
C–Rock	-1.410	0.477	6575	-2.955	0.0088
C–W	-1.896	0.302	6575	-6.284	<0.0001
Rock–W	-0.486	0.477	6575	-1.020	0.564

Table S3. Model summary table for Model S1, an autoregressive linear mixed effects model testing the effect of treatment on mean daily maximum temperature recorded by temperature loggers during daytime summer low tides of the second year of the thermal manipulation. Random intercept effects were included for individual tile and sampling date, with an autoregressive order 1 process for sampling date to reduce temporal autocorrelation. Coefficients given are relative to the cool summer – cool summer (CC) treatment, and the model was tested using a Type II ANOVA. SE = standard error, df = degrees freedom. CW = cool summer – warm summer, WC = warm summer – warm summer, WW = warm summer – warm summer.

Term	Coefficient	SE	χ^2	df	P
Intercept	27.092	0.634			
Treatment–CW	1.960	0.425			
Treatment–Rock	1.034	0.521	52.34	4	1.17 x 10⁻¹⁰
Treatment–WC	-0.010	0.425			
Treatment–WW	2.345	0.425			

Table S4 Tukey-Kramer *post hoc* comparison of the mean daily maximum temperature of treatment groups in year two of the thermal manipulation. See Table S3 for treatment codes and abbreviations.

Contrast	Estimate	SE	df	t ratio	P
CC–CW	-1.960	0.425	6580	-4.61	<0.0001
CC–Rock	-1.034	0.521	6580	-1.99	0.273
CC–WC	0.010	0.425	6580	0.024	1.00
CC–WW	-2.345	0.425	6580	-5.52	<0.0001
CW–Rock	0.927	0.521	6580	1.78	0.386
CW–WC	1.970	0.425	6580	4.63	<0.0001
CW–WW	-0.385	0.425	6580	-0.91	0.895
Rock–WC	1.044	0.521	6580	2.01	0.264
Rock–WW	-1.311	0.521	6580	-2.52	0.0866
WC–WW	-2.355	0.425	6580	-5.54	<0.0001

Model S2

Mean daily temperature \sim treatment + (1 | tile) + (1 | date) + ar1(date - 1 | tile)

Error distribution: Gaussian

Table S5. Model summary table for Model S2, an autoregressive linear mixed effects model testing the effect of treatment on daily mean temperatures recorded by temperature loggers during daytime summer low tides of the first year of the thermal manipulation. Random intercept effects were included for individual tile and sampling date, with an autoregressive order 1 process for sampling date to reduce temporal autocorrelation. Coefficients given are relative to the cool treatment, and the model was tested using a Type II ANOVA. df = degrees of freedom, SE = standard error.

Term	Coefficient	SE	χ^2	df	P
Intercept	21.415	0.452			
Treatment–Rock	1.192	0.318	37.38	2	7.62x10 ⁻⁹
Treatment–Warm	1.158	0.201			

Table S6. Tukey-Kramer *post hoc* comparison of the mean daily temperature of treatment groups in year one of the thermal manipulation. SE = standard error, C = cool treatment, W = warm treatment

Contrast	Estimate	SE	df	z ratio	P
C–Rock	-1.192	0.317	6575	-3.75	0.0005
C–W	-1.158	0.201	6575	-5.77	<0.0001
Rock–W	0.034	0.317	6575	0.11	0.994

Table S7. Model summary table for Model S2, an autoregressive linear mixed effects model testing the effect of treatment on mean daily temperature recorded by temperature loggers during daytime summer low tides of the second year of the thermal manipulation. Random intercept effects were included for individual tile and sampling date, with an autoregressive order 1 process for sampling date to reduce temporal autocorrelation. Coefficients given are relative to the cool summer – cool summer (CC) treatment, and the model was tested using a Type II ANOVA. See Table S3 for abbreviations.

Term	Coefficient	SE	χ^2	df	P
Intercept	21.449	0.465			
Treatment–CW	1.212	0.211			
Treatment–Rock	0.806	0.258	78.48	4	3.66 x 10⁻¹⁶
Treatment–WC	0.063	0.211			
Treatment–WW	1.463	0.211			

Table S8. Tukey-Kramer *post hoc* comparison of mean daily temperature of treatment groups in year two of the thermal manipulation. See Table S3 for treatment codes and abbreviations.

Contrast	Estimate	SE	df	z ratio	P
CC–CW	-1.212	0.211	6580	-5.75	<0.0001
CC–Rock	-0.806	0.258	6580	-3.12	0.0155
CC–WC	-0.063	0.211	6580	-0.298	0.998
CC–WW	-1.463	0.211	6580	-6.94	<0.0001
CW–Rock	0.406	0.258	6580	1.57	0.516
CW–WC	1.150	0.211	6580	5.45	<0.0001
CW–WW	-0.251	0.211	6580	-1.19	0.759
Rock–WC	0.744	0.258	6580	2.88	0.0326
Rock–WW	-0.656	0.258	6580	-2.54	0.0819
WC–WW	-1.400	0.211	6580	-6.64	<0.0001

Model S3

Balanus glandula recruit year 1 abundance \sim treatment_{y1} + (1|block)

Error distribution: Quasi-Poisson

Table S9. Model summary table for Model S3, a generalized linear mixed effects model of *B. glandula* recruit abundance on experimental tiles during peak recruitment in the first year of the thermal manipulation. Recruit abundance was modeled as a function of the temperature treatment, with a random effect of block. Coefficients given are relative to the cool treatment, and the model was tested using a Type II ANOVA. Treatment_{y1} = treatment in year one, SE = standard error, df = degrees of freedom

Term	Coefficient	SE	χ^2	df	<i>P</i>
Intercept	4.984	0.326			
Treatment _{y1}	0.0899	0.0769	1.37	1	0.243

Model S4

Chthamalus dalli recruit year 1 abundance \sim treatment_{y1} + (1|block)

Error distribution: Quasi-Poisson

Table S10. Model summary table for Model S4, a generalized linear mixed effects model of *C. dalli* recruit abundance on experimental tiles during peak recruitment in the first year of the thermal manipulation (June 2019). Recruit abundance was modeled in relation to the temperature treatment applied in year one, with a random effect of block Coefficients given are relative to the cool treatment, and the model was tested using a Type II ANOVA. Treatment_{y1} = treatment in year one, SE = standard error, df = degrees of freedom

Term	Coefficient	SE	χ^2	df	<i>P</i>
Intercept	1.692	0.303			
Treatment _{y1}	-0.469	0.231	4.13	1	0.0422

Model S5

Balanus glandula recruit year 2 abundance ~ treatment_{y1} * treatment_{y2} + (1|block)

Error distribution: Quasi-Poisson

Table S11. Model summary table for Model S4, a generalized linear mixed effects model of *B. glandula* recruit abundance on experimental tiles during peak recruitment in the first year of the thermal manipulation (May 2019). Recruit abundance was modeled as an interaction of the temperature treatment applied in year one and the temperature treatment applied in year two, with a random effect of block. Coefficients given are relative to the cool treatment, and the model was tested using a Type III ANOVA. Treatment_{y1} = treatment in year one, treatment_{y2} = treatment in year two, SE = standard error, df = degrees of freedom

Term	Coefficient	SE	χ^2	df	P
Intercept	4.934	0.159			
Treatment _{y1}	-0.3884	0.1576	6.07	1	0.0138
Treatment _{y2}	-1.301	0.210	38.34	1	5.94x10⁻¹⁰
Treatment _{y1} * Treatment _{y2}	0.3537	0.2900	1.49	1	0.223

Table S12. Tukey-Kramer *post hoc* comparison of *B. glandula* recruitment between treatment groups in year two of the thermal manipulation. See Table S3 for treatment codes and abbreviations.

Contrast	Estimate	SE	df	z ratio	P
CC–WC	0.388	0.158	Inf	2.46	0.0657
CC–CW	1.301	0.210	Inf	6.19	<0.0001
CC–WW	1.335	0.193	Inf	6.91	<0.0001
WC–CW	0.912	0.220	Inf	4.15	0.0002
WC–WW	0.947	0.206	Inf	4.60	<0.0001
CW–WW	0.035	0.242	Inf	0.14	0.999

Model S6

Chthamalus dalli recruit year 2 abundance ~ treatment_{y1} * treatment_{y2} + (1|block)

Error distribution: Quasi-Poisson

Table S13. Model summary table for Model S6, a generalized linear mixed effects model of *B. glandula* recruit abundance on experimental tiles during peak recruitment in the first year of the thermal manipulation. Recruit abundance was modeled as an interaction of the temperature treatment applied in year one and the temperature treatment applied in year two, with a random effect of block. Coefficients given are relative to the cool treatment, and the model was tested using a Type III ANOVA. Treatment_{y1} = treatment in year one, treatment_{y2} = treatment in year two, SE = standard error, df = degrees of freedom

Term	Coefficient	SE	χ^2	df	P
Intercept	3.347	0.208			
Treatment _{y1}	-0.392	0.166	5.56	1	0.0184
Treatment _{y2}	-0.852	0.195	19.16	1	1.20x10⁻⁵
Treatment _{y1} * Treatment _{y2}	0.430	0.272	2.50	1	0.114

Table S14. Tukey-Kramer *post hoc* comparison of *C. dalli* recruitment between treatment groups in year two of the thermal manipulation. See Table S3 for treatment codes and abbreviations.

Contrast	Estimate	SE	df	z ratio	P
CC–WC	0.392	0.158	Inf	2.36	0.0856
CC–CW	0.852	0.195	Inf	4.38	0.0001
CC–WW	0.815	0.178	Inf	4.58	<0.0001
WC–CW	0.460	0.208	Inf	2.22	0.119
WC–WW	0.423	0.192	Inf	2.20	0.124
CW–WW	-0.038	0.215	Inf	-0.18	0.998

Model S7

Balanus glandula year 1 adult abundance ~ treatment_{y1} + (1|block)

Error distribution: Quasi-Poisson

Table S15. Model summary table for Model S7, a generalized linear mixed effects model of adult *B. glandula* abundance on experimental tiles at the end of the first year of the thermal manipulation. Barnacle abundance was modeled in relation to the temperature treatment applied in year one, with a random effect of block. Coefficients given are relative to the cool treatment, and the model was tested using a Type II ANOVA. Treatment_{y1} = treatment in year one, SE = standard error, df = degrees of freedom

Term	Coefficient	SE	χ^2	df	P
Intercept	3.237	0.275			
Treatment _{y1}	-1.524	0.148	106.20	1	<2.2x10 ⁻¹⁶

Model S8

Balanus glandula year 2 adult abundance ~ treatment_{y1} * treatment_{y2} + (1|block)

Error distribution: Quasi-Poisson

Table S16. Model summary table for Model S8, a generalized linear mixed effects model of adult *B. glandula* abundance on experimental tiles at the end of the second year of the thermal manipulation. Barnacle abundance was modeled as an interaction of the temperature treatment applied in year one and the temperature treatment applied in year two, with a random effect of block. Coefficients given are relative to the cool treatment, and the model was tested using a Type III ANOVA. Treatment_{y1} = treatment in year one, treatment_{y2} = treatment in year two, SE = standard error, df = degrees of freedom

Term	Coefficient	SE	χ^2	df	P
Intercept	3.487	0.379			
Treatment _{y1}	-0.822	0.477	2.97	1	0.0846
Treatment _{y2}	-0.807	0.505	2.55	1	0.110
Treatment _{y1} * Treatment _{y2}	0.156	0.715	0.048	1	0.827

Table S17. Tukey-Kramer *post hoc* comparison of adult *B. glandula* abundance between treatment groups in year two of the thermal manipulation. See Table S3 for treatment codes and abbreviations.

Contrast	Estimate	SE	df	z ratio	P
CC–WC	0.822	0.477	Inf	1.73	0.311
CC–CW	0.807	0.505	Inf	1.60	0.380
CC–WW	1.473	0.478	Inf	3.08	0.0111
WC–CW	-0.016	0.551	Inf	-0.028	1.00
WC–WW	0.651	0.525	Inf	1.24	0.601
CW–WW	0.666	0.535	Inf	1.25	0.598

Model S9

Balanus glandula mortality (%) ~ treatment_{y1} + (1|block/number)

Error distribution: Tweedie

Table S18. Model summary table for Model S9, a generalized linear mixed effects model of *B. glandula* mortality on experimental tiles on 27 August 2019, during the first year of the thermal manipulation. Barnacle abundance was modeled in relation to the temperature treatment applied in year one, with a random effect of individual tile. Coefficients given are relative to the cool treatment, and the model was tested using a Type II ANOVA. Treatment_{y1} = treatment in year one, SE = standard error, df = degrees of freedom

Term	Coefficient	SE	χ^2	df	<i>P</i>
Intercept	2.367	0.314			
Treatment _{y1}	1.573	0.275	32.63	1	1.11 x 10⁻⁸

Model S10

Balanus glandula mortality (%) ~ treatment_{y1} * treatment_{y2} + date + (1|block/number)

Error distribution: Tweedie

Table S19. Model summary table for Model S10, a generalized linear mixed effects model of adult *C. dalli* abundance on experimental tiles at the end of the second year of the thermal manipulation. Barnacle abundance was modeled as an interaction of the temperature treatment applied in year one and the temperature treatment applied in year two plus an additive term for sampling date, with a random effect of block. Coefficients given are relative to the consistently cool treatment, and the model was tested using a Type III ANOVA. Treatment_{y1} = treatment in year one, treatment_{y2} = treatment in year two, SE = standard error, df = degrees of freedom

Term	Coefficient	SE	χ^2	df	P
Intercept	0.992	0.355			
Treatment _{y1}	-0.082	0.460	0.03	1	0.859
Treatment _{y2}	1.556	0.440	12.48	1	4.12x10⁻⁴
Date: 2020-09-14	0.169	0.219			
Date: 2020-12-11	0.216	0.316	1.07	2	0.585
Treatment _{y1} * Treatment _{y2}	-1.471	0.663	4.93	1	0.0264

Model S11

Log (*Balanus glandula* basal diameter) \sim treatment_{y1} + (1|block/number)

Error distribution: Gaussian

Table S20. Model summary table for Model S11, a generalized linear mixed effects model of *B. glandula* size on experimental tiles on 27 August 2019, during the first year of the thermal manipulation. Barnacle abundance was modeled in relation to the temperature treatment applied in year one, with a random effect of individual tile. Coefficients given are relative to the cool treatment, and the model was tested using a Type II ANOVA. Treatment_{y1} = treatment in year one, SE = standard error, df = degrees of freedom

Term	Coefficient	SE	F	df	df (residuals)	P
Intercept	1.519	0.029				
Treatment _{y1}	-0.349	0.050	25.09	1	98	2.41 x 10⁻⁶

Model S12

Log (*Balanus glandula* basal diameter) ~ treatment_{y1} * treatment_{y2} * date + (1|block/number)
Error distribution: Gaussian

Table S21. Model summary table for Model S12, a generalized linear mixed effects model of adult *B. glandula* size on experimental tiles at the end of the second year of the thermal manipulation. Barnacle size was modeled as an interaction of the temperature treatment applied in year one and the temperature treatment applied in year two and the date on which data were collected, with a random effect of block Coefficients given are relative to the cool treatment (for treatment) and tiles on 9 July 2020 (for date), and the model was tested using a Type III ANOVA. Treatment_{y1} = treatment in year one, treatment_{y2} = treatment in year two, SE = standard error, df = degrees of freedom

Term	Coefficient	SE	F	df	df (residuals)	P
Intercept	1.866	0.082				
Treatment _{y1}	-0.188	0.068	7.60	1	89	0.00710
Treatment _{y2}	-0.047	0.703	0.42	1	103	0.517
Date: 2020-09-14	-0.019	0.027	2.07	2	1516	0.127
Date: 2020-12-11	0.047	0.033				
Treatment _{y1} * Treatment _{y2}	-0.336	0.105	10.21	1	83	0.00193
Treatment _{y1} * Date: 2020-09-14	0.071	0.040	4.62	2	1518	0.0100
Treatment _{y1} * Date: 2020-12-11	0.146	0.050				
Treatment _{y2} * Date: 2020-09-14	0.028	0.048	1.01	2	1554	0.363
Treatment _{y2} * Date: 2020-12-11	-0.060	0.061				
Treatment _{y1} * Treatment _{y2} * Date: 2020-09-14	0.246	0.066	6.92	2	1552	0.00102
Treatment _{y1} * Treatment _{y2} * Date: 2020-12-11	0.125	0.081				

Model S13

Chthamalus dalli year 1 adult abundance \sim treatment_{y1} + (1|block)

Error distribution: Quasi-Poisson

Table S22. Model summary table for Model S13, a generalized linear mixed effects model of adult *C. dalli* abundance on experimental tiles at the end of the first year of the thermal manipulation. Barnacle abundance was modeled in relation to temperature treatment applied in year one, with a random effect of block. Coefficients given are relative to the cool treatment, and the model was tested using a Type II ANOVA. Treatment_{y1} = treatment in year one, SE = standard error, df = degrees of freedom

Term	Coefficient	SE	χ^2	df	<i>P</i>
Intercept	-1.654	0.572			
Treatment _{y1}	-0.287	0.356	0.65	1	0.420

Model S14

Chthamalus dalli year 2 adult abundance ~ treatment_{y1} * treatment_{y2} + (1|block)

Error distribution: Quasi-Poisson

Table S23. Model summary table for Model S14, a generalized linear mixed effects model of adult *C. dalli* abundance on experimental tiles at the end of the second year of the thermal manipulation. Barnacle abundance was modeled as an interaction of the temperature treatment applied in year one and the temperature treatment applied in year two, with a random effect of block. Coefficients given are relative to the cool treatment, and the model was tested using a Type III ANOVA. Treatment_{y1} = treatment in year one, treatment_{y2} = treatment in year two, SE = standard error, df = degrees of freedom

Term	Coefficient	SE	χ^2	df	P
Intercept	3.080	0.408			
Treatment _{y1}	-0.502	0.462	1.18	1	0.277
Treatment _{y2}	-0.239	0.490	0.24	1	0.626
Treatment _{y1} * Treatment _{y2}	-0.139	0.685	0.041	1	0.840

Table S24. Tukey-Kramer *post hoc* comparison of adult *C. dalli* abundance between treatment groups in year two of the thermal manipulation. See Table S3 for treatment codes and abbreviations.

Contrast	Estimate	SE	df	z ratio	P
CC–WC	0.502	0.462	Inf	1.09	0.698
CC–CW	0.239	0.490	Inf	0.49	0.962
CC–WW	0.879	0.450	Inf	1.95	0.207
WC–CW	-0.263	0.518	Inf	-0.51	0.957
WC–WW	0.377	0.487	Inf	0.77	0.866
CW–WW	0.641	0.500	Inf	1.28	0.575

Model S15

Lottia spp. abundance \sim treatment_{y1} * treatment_{y2} + (1|block)

Error distribution: Quasi-Poisson

Table S25. Model summary table for Model S15, a generalized linear mixed effects model of *Lottia* spp. abundance on experimental tiles at the end of the second summer, on 14 September 2020. Limpet abundance was modeled as an interaction of the temperature treatment applied in year one and the temperature treatment applied in year two, with a random effect of block. Coefficients for treatment are given are relative to the cool treatment, and the model was tested using a Type III ANOVA. Treatment_{y1} = treatment in year one, treatment_{y2} = treatment in year two, SE = standard error, df = degrees of freedom

Term	Coefficient	SE	χ^2	df	P
Intercept	0.498	0.532			
Treatment _{y1}	-0.294	0.191	2.36	1	0.124
Treatment _{y2}	-0.781	0.235	11.07	1	8.77 x 10⁻⁴
Treatment _{y1} * Treatment _{y2}	0.102	0.342	0.09	1	0.766

Table S26. Tukey-Kramer *post hoc* comparison of *Lottia* spp. abundance between treatment groups at the end of summer in year two of the thermal manipulation. See Table S3 for treatment codes and abbreviations.

Contrast	Estimate	SE	df	z ratio	P
CC–WC	0.294	0.191	Inf	1.54	0.416
CC–CW	0.781	0.235	Inf	3.33	0.0049
CC–WW	0.973	0.236	Inf	4.12	0.0002
WC–CW	0.487	0.249	Inf	1.96	0.204
WC–WW	0.679	0.250	Inf	2.72	0.0333
CW–WW	0.192	0.284	Inf	0.676	0.906

Table S26. Model summary table for Model S15, a generalized linear mixed effects model of *Lottia* spp. abundance on experimental tiles at the end of the second winter, on 24 February 2021. Limpet abundance was modeled as an interaction of the temperature treatment applied in year one and the temperature treatment applied in year two, with a random effect of block. Coefficients for treatment are given are relative to the cool treatment, and the model was tested using a Type III ANOVA. Treatment_{y1} = treatment in year one, treatment_{y2} = treatment in year two, SE = standard error, df = degrees of freedom

Term	Coefficient	SE	χ^2	df	P
Intercept	1.733	0.528			
Treatment _{y1}	-0.621	0.328	3.57	1	0.0587
Treatment _{y2}	-0.744	0.494	2.27	1	0.132
Treatment _{y1} * Treatment _{y2}	-1.186	0.865	1.88	1	0.170

Table S27. Tukey-Kramer *post hoc* comparison of *Lottia* spp. abundance between treatment groups at the end of the winter in year two of the thermal manipulation. See Table S3 for treatment codes and abbreviations.

Contrast	Estimate	SE	df	z ratio	P
CC–WC	0.621	0.328	Inf	1.89	0.232
CC–CW	0.744	0.494	Inf	1.51	0.434
CC–WW	2.551	0.740	Inf	3.45	0.0032
WC–CW	0.123	0.516	Inf	0.24	0.995
WC–WW	1.930	0.749	Inf	2.58	0.0492
CW–WW	1.807	0.805	Inf	2.25	0.111

Model S16

Littorina spp. abundance \sim treatment_{y1} * treatment_{y2} + (1|block)

Error distribution: Quasi-Poisson

Table S28. Model summary table for Model S16, a generalized linear mixed effects model of *Littorina* spp. abundance on experimental tiles at the end of the second summer, on 14 September 2020. Littorine abundance was modeled as an interaction of the temperature treatment applied in year one and the temperature treatment applied in year two, with a random effect of block. Coefficients given are relative to the cool treatment, and the model was tested using a Type III ANOVA. Treatment_{y1} = treatment in year one, treatment_{y2} = treatment in year two, SE = standard error, df = degrees of freedom

Term	Coefficient	SE	χ^2	df	P
Intercept	4.094	0.205			
Treatment _{y1}	-1.045	0.249	17.56	1	2.79 x 10⁻⁵
Treatment _{y2}	-0.909	0.224	13.38	1	2.54 x 10⁻⁴
Treatment _{y1} * Treatment _{y2}	0.482	0.374	1.66	1	0.198

Table S29. Tukey-Kramer *post hoc* comparison of *Littorina* spp. abundance between treatment groups at the end of summer in year two of the thermal manipulation. See Table S3 for treatment codes and abbreviations.

Contrast	Estimate	SE	df	z ratio	P
CC–WC	1.045	0.249	Inf	4.19	0.0002
CC–CW	0.909	0.248	Inf	3.66	0.0014
CC–WW	1.473	0.256	Inf	5.76	<0.0001
WC–CW	-0.136	0.283	Inf	-0.48	0.963
WC–WW	0.427	0.282	Inf	1.52	0.428
CW–WW	0.563	0.286	Inf	1.97	0.199

Table S30. Model summary table for Model S16, a generalized linear mixed effects model of *Littorina* spp. abundance on experimental tiles at the end of the second winter, on 24 February 2021. Limpet abundance was modeled as an interaction of the temperature treatment applied in year one and the temperature treatment applied in year two, with a random effect of block. Coefficients given are relative to the cool treatment, and the model was tested using a Type III ANOVA. Treatment_{y1} = treatment in year one, treatment_{y2} = treatment in year two, SE = standard error, df = degrees of freedom

Term	Coefficient	SE	χ^2	df	P
Intercept	2.379	0.347			
Treatment _{y1}	-0.916	0.505	3.29	1	0.0698
Treatment _{y2}	-1.159	0.589	3.87	1	0.0491
Treatment _{y1} * Treatment _{y2}	-0.571	1.000	0.326	1	0.568

Table S31. Tukey-Kramer *post hoc* comparison of *Littorina* spp. abundance between treatment groups at the end of winter in year two of the thermal manipulation. See Table S3 for treatment codes and abbreviations.

Contrast	Estimate	SE	df	z ratio	P
CC–WC	0.916	0.505	Inf	1.81	0.267
CC–CW	1.159	0.589	Inf	1.97	0.200
CC–WW	2.646	0.776	Inf	3.41	0.0036
WC–CW	0.243	0.639	Inf	0.38	0.981
WC–WW	1.730	0.814	Inf	2.12	0.145
CW–WW	1.487	0.863	Inf	1.72	0.311

Model S17

Algal cover (%) ~ treatment + s(time) + s(time, by = treatment) + s(block, type = "re")

Error distribution: Gaussian

Correlation: AR(1) process

Table S32. Model summary table for Model S17, a generalized additive mixed model of differences in algal cover over time between treatments in the first year of the experiment (after 27 August 2019). Algal cover was modeled in relation to treatment and smoothed effects of time (days since experiment start) within each treatment, with a random effect of block and an AR(1) process to account for autocorrelation of the residuals. Estimates and differences between smooth functions are given relative to the cool treatment. SE = standard error, edf = effective degrees of freedom, W = warm treatment.

Component	Term	Estimate	SE	t	P
Linear	Intercept	17.241	3.043		
	Treatment: W	6.943	2.101	3.30	0.00109
		edf		F	P
Smooth	s(time)	1.92		29.60	<2x10⁻¹⁶
	s(time):W	1.49		30.33	3.64x10⁻⁷
	s(block)	2.68		1.12	0.0678

Model S18

Algal cover (%) ~ treatment_{y1} * treatment_{y2} + s(time) + s(time, by = treatment)
+ s(block, type = “re”)

Error distribution: Gaussian

Correlation: AR(1) process

Table S33. Model summary table for Model S18, a generalized additive mixed model of differences in algal cover over time between treatments in the second year of the experiment. Algal cover was modeled in relation to the interactive effect of treatment in year one and treatment in year two and smoothed effects of time (days since the experiment start) within each treatment, with a random effect of block and an AR(1) process to account for autocorrelation of the residuals. Estimates and differences between smooth functions are given relative to the cool treatment. k=5 for smoothing functions of time. Treatment_{y1} = treatment in year one, treatment_{y2} = treatment in year two, SE = standard error, edf = effective degrees of freedom. See Table S3 for treatment codes.

Component	Term	Estimate	SE	t	P
Linear	Intercept	2.456	1.135		
	Treatment _{y1}	1.322	1.077	1.23	0.220
	Treatment _{y2}	3.116	1.141	2.73	0.00656
	Treatment _{y1} * Treatment _{y2}	-3.867	1.504	-2.57	0.0104
		edf		F	P
Smooth	s(time)	3.73		6.57	0.00466
	s(time):CW	3.44		5.88	0.00204
	s(time):WC	2.40		9.12	4 x 10⁻⁵
	s(time):WW	1.00		3.71	0.0548
	s(block)	0.40		0.09	0.361

Model S19

Species richness \sim treatment_{y1} + (1|block)

Error distribution: Poisson

Table S34. Model summary table for Model S19, a generalized linear mixed effects model of the species richness on experimental tile communities at the end of the first summer, on 20 October 2019. Species richness was modeled under a Poisson distribution as a function of treatment, with block included as a random intercept effect. Coefficients given are relative to the cool treatment, and the model was tested using a Type II ANOVA. Treatment_{y1} = treatment in year one, SE = standard error, df = degrees of freedom.

Term	Coefficient	SE	χ^2	df	<i>P</i>
Intercept	1.386	0.083			
Treatment _{y1}	-0.468	0.116	16.33	1	5.32 x 10⁻⁵

Table S35. Model summary table for Model S19, a generalized linear mixed effects model of the species richness on experimental tile communities at the end of the first winter, on 15 March 2020. Species richness was modeled under a Poisson distribution as a function of treatment, with block included as a random intercept effect. Coefficients given are relative to the cool treatment, and the model was tested using a Type II ANOVA. Treatment_{y1} = treatment in year one, SE = standard error, df = degrees of freedom.

Term	Coefficient	SE	χ^2	df	<i>P</i>
Intercept	1.138	0.189			
Treatment _{y1}	-0.959	0.111	74.85	1	<2.2 x 10⁻¹⁶

Model S20

$\text{Log}(\text{Species richness} + 1) \sim \text{treatment}_{y1} * \text{treatment}_{y2} + (1|\text{block})$

Error distribution: Gaussian

Table S36. Model summary table for Model S20, a linear mixed effects model of the species richness of experimental tiles at the end of the second summer, on 14 September 2020. Species richness was log-transformed and modeled under a normal distribution in relation to the interaction of treatments in year one and year two, with block included as a random effect. Coefficients given are relative to the cool treatment, and the model was tested using a Type III ANOVA. Treatment_{y1} = treatment in year one, treatment_{y2} = treatment in year two, SE = standard error, df = degrees of freedom.

Term	Coefficient	SE	χ^2	df	P
Intercept	1.814	0.044			
Treatment _{y1}	-0.078	0.061	1.61	1	0.204
Treatment _{y2}	-0.137	0.063	4.73	1	0.0297
Treatment _{y1} * Treatment _{y2}	-0.065	0.086	0.57	1	0.450

Table S37. Tukey-Kramer *post hoc* comparison of species richness between treatment groups at the end of summer in year two of the thermal manipulation. See Table S3 for treatment codes and abbreviations.

Contrast	Estimate	SE	df	t ratio	P
CC–WC	0.078	0.061	78	1.22	0.585
CC–CW	0.137	0.063	78	2.17	0.140
CC–WW	0.280	0.059	78	4.78	<0.001
WC–CW	0.059	0.064	78	0.93	0.790
WC–WW	0.202	0.059	78	3.42	0.0054
CW–WW	0.143	0.061	78	2.35	0.0967

Model S21

Species richness \sim treatment_{y1} * treatment_{y2} + (1|block)

Error distribution: Gaussian

Table S38. Model summary table for Model S21, a generalized linear mixed effects model of the species richness of experimental tiles at the end of the second winter, on 24 February 2021.

Species richness was modeled under a Poisson distribution in relation to the interaction of treatments in year one and year two, with block included as a random effect. Coefficients given are relative to the cool treatment, and the model was tested using a Type III ANOVA.

Treatment_{y1} = treatment in year one, treatment_{y2} = treatment in year two, SE = standard error, df = degrees of freedom.

Term	Coefficient	SE	χ^2	df	P
Intercept	1.655	0.180			
Treatment _{y1}	-0.106	0.185	0.33	1	0.566
Treatment _{y2}	-0.300	0.228	1.73	1	0.188
Treatment _{y1} * Treatment _{y2}	-0.417	0.312	1.79	1	0.181

Table S39. Tukey-Kramer *post hoc* comparison of species richness between treatment groups at the end of winter in year two of the thermal manipulation. See Table S3 for treatment codes and abbreviations.

Contrast	Estimate	SE	df	z ratio	P
CC–WC	0.106	0.185	Inf	0.57	0.940
CC–CW	0.300	0.228	Inf	1.32	0.552
CC–WW	0.824	0.213	Inf	3.87	0.0006
WC–CW	0.194	0.233	Inf	0.83	0.839
WC–WW	0.717	0.219	Inf	3.27	0.0059
CW–WW	0.524	0.250	Inf	2.09	0.156

Model S22

Invertebrate Shannon diversity \sim treatment_{y1} + (1|block)

Error distribution: Tweedie

Dispersion formula: \sim treatment_{y1}

Table S40. Model summary table for Model S22, a generalized linear mixed effects model of the invertebrate Shannon diversity of experimental tile communities at the end of the first summer, on 20 October 2019. Invertebrate Shannon diversity was modeled under a Tweedie distribution in relation to the treatment in year one, with block included as a random effect. Coefficients given are relative to the cool treatment, and the model was tested using a Type II ANOVA. Treatment_{y1} = treatment in year one, treatment_{y2} = treatment in year two, SE = standard error, df = degrees of freedom.

Term	Coefficient	SE	χ^2	df	<i>P</i>
Intercept	-1.017	0.115			
Treatment _{y1}	-0.085	0.244	0.122	1	0.727
Dispersion model					
Intercept	-1.505	0.162			
Treatment _{y1}	1.363	0.181			

Table S41. Model summary table for Model S22, a generalized linear mixed effects model of the invertebrate Shannon diversity of experimental tile communities at the end of the first winter, on 15 March 2020. Invertebrate Shannon diversity was modeled under a Tweedie distribution in relation to the treatment in year one, with block included as a random effect. Coefficients given are relative to the cool treatment, and the model was tested using a Type II ANOVA. See Table S3 for abbreviations.

Term	Coefficient	SE	χ^2	df	<i>P</i>
Intercept	-1.351	0.425			
Treatment _{y1}	-1.401	0.271	26.67	1	2.41 x 10⁻⁷
Dispersion model					
Intercept	-1.500	0.075			
Treatment _{y1}	0.987	0.098			

Model S23

Invertebrate Shannon diversity \sim treatment_{y1} * treatment_{y2} + (1|block)

Error distribution: Tweedie

Table S42. Model summary table for Model S23, a generalized linear mixed effects model of the invertebrate Shannon diversity of experimental tiles at the end of the second summer, on 14 September 2020. Invertebrate Shannon diversity was modeled under a Tweedie distribution in relation to the interaction of treatments in year one and year two, with block included as a random effect. Coefficients given are relative to the cool treatment, and the model was tested using a Type III ANOVA. Treatment_{y1} = treatment in year one, treatment_{y2} = treatment in year two, SE = standard error, df = degrees of freedom.

Term	Coefficient	SE	χ^2	df	P
Intercept	1.200	0.054			
Treatment _{y1}	-0.200	0.074	7.35	1	0.00669
Treatment _{y2}	-0.109	0.076	2.07	1	0.150
Treatment _{y1} * Treatment _{y2}	-0.010	0.104	0.0097	1	0.921

Table S43. Tukey-Kramer *post hoc* comparison of invertebrate Shannon diversity between treatment groups at the end of the second summer of the thermal manipulation. See Table S3 for treatment codes and abbreviations.

Contrast	Estimate	SE	df	t ratio	P
CC–WC	0.200	0.074	78	2.71	0.0402
CC–CW	0.109	0.076	78	1.44	0.479
CC–WW	0.319	0.070	78	4.56	0.0001
WC–CW	-0.090	0.077	78	-1.18	0.642
WC–WW	0.119	0.071	78	1.69	0.338
CW–WW	0.210	0.073	78	2.88	0.0261

Table S44. Model summary table for Model S23, a generalized linear mixed effects model of the invertebrate Shannon diversity of experimental tiles at the end of the second winter, on 24 February 2021. Invertebrate Shannon diversity was modeled under a Tweedie distribution in relation to the interaction of treatments in year one and year two, with block included as a random effect. Coefficients given are relative to the cool treatment, and the model was tested using a Type III ANOVA. Treatment_{y1} = treatment in year one, treatment_{y2} = treatment in year two, SE = standard error, df = degrees of freedom.

Term	Coefficient	SE	χ^2	df	P
Intercept	0.964	0.139			
Treatment _{y1}	-0.318	0.169	3.52	1	0.0605
Treatment _{y2}	-0.214	0.189	1.28	1	0.258
Treatment _{y1} * Treatment _{y2}	-0.046	0.245	0.04	1	0.851

Table S45. Tukey-Kramer *post hoc* comparison of invertebrate Shannon diversity between treatment groups at the end of the second winter of the thermal manipulation. See Table S3 for treatment codes and abbreviations.

Contrast	Estimate	SE	df	t ratio	P
CC–WC	0.318	0.169	41	1.88	0.254
CC–CW	0.214	0.189	41	1.13	0.673
CC–WW	0.578	0.159	41	3.62	0.0042
WC–CW	-0.104	0.190	41	-0.55	0.947
WC–WW	0.260	0.161	41	1.61	0.383
CW–WW	0.364	0.177	41	2.05	0.186

Model S24

Algal Shannon diversity \sim treatment_{y1} + (1|block)

Error distribution: Tweedie

Table S46. Model summary table for Model S24, a generalized linear mixed effects model of the algal Shannon diversity of experimental tile communities for data collected at the end of the first winter, on 15 March 2020. Algal Shannon diversity was modeled under a Tweedie distribution as a function of treatment during the first year, with block included as a random intercept effect. Coefficients given are relative to the cool treatment, and the model was tested using a Type II ANOVA. Treatment_{y1} = treatment in year one, SE = standard error, df = degrees of freedom.

Term	Coefficient	SE	χ^2	df	<i>P</i>
Intercept	-2.507	0.651			
Treatment _{y1}	-1.855	0.602	9.48	1	0.00208

Model S25

Algal Shannon diversity \sim treatment_{y1} * treatment_{y2} + (1|block)

Error distribution: Tweedie

Table S47. Model summary table for Model S25, a generalized linear mixed effects model of the algal Shannon diversity of experimental tiles at the end of the second winter, on 24 February 2021. Algal Shannon diversity was modeled under a Tweedie distribution in relation to the interaction of treatments in year one and year two, with block included as a random effect. Coefficients given are relative to the cool treatment, and the model was tested using a Type III ANOVA. Treatment_{y1} = treatment in year one, treatment_{y2} = treatment in year two, SE = standard error, df = degrees of freedom.

Term	Coefficient	SE	χ^2	df	P
Intercept	-1.609	0.507			
Treatment _{y1}	0.7698	0.6407	1.444	1	0.230
Treatment _{y2}	-0.3348	0.8722	0.147	1	0.701
Treatment _{y1} * Treatment _{y2}	-1.105	1.114	0.984	1	0.321

Table S48. Tukey-Kramer *post hoc* comparison of algal Shannon diversity between treatment groups at the end of winter in year two of the thermal manipulation. See Table S3 for treatment codes and abbreviations.

Contrast	Estimate	SE	df	z ratio	P
CC–WC	-0.770	0.641	Inf	-1.20	0.626
CC–CW	0.335	0.872	Inf	0.38	0.981
CC–WW	0.670	0.765	Inf	0.88	0.818
WC–CW	1.105	0.810	Inf	1.35	0.522
WC–WW	1.440	0.693	Inf	2.08	0.161
CW–WW	0.335	0.912	Inf	0.37	0.983

Model S26

Species assemblage \sim treatment_{y1} * treatment_{y2}

Table S49. Model summary table of PERMANOVA output for Model S26 describing differences in epifaunal community composition of experimental tiles destructively sampled on 14 September 2020. PERMANOVA used constrained ordination within experimental blocks via distance-based redundancy analyses with Bray-Curtis distances. Community structure was modeled in relation the interaction of treatment of year one and treatment in year two. Treatment_{y1} = treatment in year one, treatment_{y2} = treatment in year two, df = degrees of freedom.

Term	df	Sum of squares	F	P
Treatment _{y1}	1	0.434	1.69	0.0825
Treatment _{y2}	1	0.389	1.51	0.120
Treatment _{y1} * Treatment _{y2}	1	0.329	1.28	0.192
Residuals	31	7.952		

Table S50. Multiple pairwise comparisons of epifaunal community composition across treatments using constrained ordination via distance-based redundancy analyses with Bray-Curtis distances. Epifauna were destructively sampled on 14 September 2020. See Table S3 for treatment codes and abbreviations.

Comparison	df	Sum of squares	F	P
CC – CW	1	0.283	1.20	0.280
CC – WC	1	0.288	1.25	0.246
CC – WW	1	0.777	2.68	0.018
CW – WC	1	0.047	0.21	0.990
CW – WW	1	0.454	1.59	0.159
WC – WW	1	0.435	1.58	0.138

Table S51. Model summary table of PERMANOVA output for Model S26 describing differences in epifaunal community composition of experimental tiles destructively sampled on 24 February 2021. PERMANOVA used constrained ordination within experimental blocks via distance-based redundancy analyses with Bray-Curtis distances. Community structure was modeled in relation the interaction of treatment of year one and treatment in year two. Treatment_{y1} = treatment in year one, treatment_{y2} = treatment in year two, df = degrees of freedom.

Term	df	Sum of squares	F	P
Treatment _{y1}	1	0.674	2.39	0.0141
Treatment _{y2}	1	1.030	3.66	0.0015
Treatment _{y1} * Treatment _{y2}	1	0.626	2.22	0.0125
Residuals	37	10.410		

Table S52. Multiple pairwise comparisons of epifaunal community composition across treatments using constrained ordination via distance-based redundancy analyses with Bray-Curtis distances. Epifauna were destructively sampled on 24 February 2021. See Table S3 for treatment codes and abbreviations.

Comparison	df	Sum of squares	F	P
CC – CW	1	0.834	3.34	0.003
CC – WC	1	0.617	2.29	0.017
CC – WW	1	1.600	5.74	0.001
CW – WC	1	0.111	0.39	0.942
CW – WW	1	0.486	1.64	0.147
WC – WW	1	0.821	2.69	0.005

Model S27

Species assemblage heterogeneity ~ treatment

Table S53. Model summary table of PERMDISP output for Model S27 of differences in epifaunal community composition heterogeneity of experimental tiles destructively sampled in September 2020. df = degrees of freedom.

Term	df	Sum of squares	Mean squares	F	<i>P</i>
Treatment	3	0.0714	0.0238	2.58	0.0714
Residuals	31	0.2862	0.0092		

Table S54. Model summary table of PERMDISP output for Model S27 of differences in epifaunal community composition heterogeneity of experimental tiles destructively sampled in February 2021. df = degrees of freedom.

Variable	df	Sum of squares	Mean squares	F	<i>P</i>
Treatment	3	0.0440	0.0147	0.946	0.428
Residuals	37	0.5732	0.0155		

Model S28

Species richness \sim treatment_{y1} * treatment_{y2} + (1 | block)

Error distribution: Poisson

Table S55. Model summary table for Model S28, a generalized linear mixed effects model of the species richness of epifauna from destructively sampled tile communities collected on 14 September 2020. Species richness was modeled under a Poisson distribution in relation to the interaction of treatments in year one and year two, with block included as a random effect. Coefficients given are relative to the cool treatment, and the model was tested using a Type III ANOVA. Treatment_{y1} = treatment in year one, treatment_{y2} = treatment in year two, df = degrees of freedom.

Term	Coefficient	SE	χ^2	df	P
Intercept	2.291	0.106			
Treatment _{y1}	-0.107	0.154	0.48	1	0.489
Treatment _{y2}	-0.244	0.165	2.17	1	0.141
Treatment _{y1} * Treatment _{y2}	-0.187	0.243	0.59	1	0.442

Table S56. Tukey-Kramer *post hoc* comparison of species richness of epifauna from destructively sampled tile communities between treatment groups at the end of the second summer of the thermal manipulation. See Table S3 for treatment codes and abbreviations.

Contrast	Estimate	SE	df	z ratio	P
CC–WC	0.107	0.154	Inf	0.69	0.900
CC–CW	0.244	0.165	Inf	1.47	0.454
CC–WW	0.537	0.175	Inf	3.08	0.0112
WC–CW	0.137	0.169	Inf	0.81	0.850
WC–WW	0.431	0.178	Inf	2.42	0.0736
CW–WW	0.294	0.188	Inf	1.56	0.401

Table S57. Model summary table for Model S28, a generalized linear mixed effects model of the species richness of epifauna from destructively sampled tile communities collected on 24 February 2021. Species richness was modeled under a Poisson distribution in relation to the interaction of treatments in year one and year two, with block included as a random effect. Coefficients given are relative to the cool treatment, and the model was tested using a Type III ANOVA. Treatment_{y1} = treatment in year one, treatment_{y2} = treatment in year two, df = degrees of freedom.

Term	Coefficient	SE	χ^2	df	P
Intercept	2.423	0.120			
Treatment _{y1}	-0.258	0.135	3.64	1	0.0565
Treatment _{y2}	-0.316	0.168	3.55	1	0.0595
Treatment _{y1} * Treatment _{y2}	-0.161	0.233	0.48	1	0.488

Table S58. Tukey-Kramer *post hoc* comparison of species richness of epifauna from destructively sampled tile communities between treatment groups at the end of the second winter of the thermal manipulation. See Table S3 for treatment codes and abbreviations.

Contrast	Estimate	SE	df	z ratio	P
CC–WC	0.259	0.135	Inf	1.91	0.225
CC–CW	0.316	0.167	Inf	1.89	0.235
CC–WW	0.735	0.158	Inf	4.66	<0.0001
WC–CW	0.058	0.171	Inf	0.34	0.987
WC–WW	0.477	0.164	Inf	2.90	0.0193
CW–WW	0.420	0.187	Inf	2.25	0.111

Model S29

Shannon diversity \sim treatment_{y1} * treatment_{y2} + (1 | block)

Error distribution: Gaussian

Table S59. Model summary table for Model S29, a generalized linear mixed effects model of the Shannon diversity of epifauna from destructively sampled tile communities collected on 14 September 2020. Shannon diversity was modeled under a Tweedie distribution in relation to the interaction of treatments in year one and year two, with block included as a random effect. Coefficients given are relative to the cool treatment, and the model was tested using a Type III ANOVA. Treatment_{y1} = treatment in year one, treatment_{y2} = treatment in year two, df = degrees of freedom.

Term	Coefficient	SE	χ^2	df	P
Intercept	1.358	0.116			
Treatment _{y1}	-0.061	0.165	0.14	1	0.710
Treatment _{y2}	-0.248	0.170	2.14	1	0.144
Treatment _{y1} * Treatment _{y2}	-0.346	0.236	2.14	1	0.144

Table S60. Tukey-Kramer *post hoc* comparison of the Shannon diversity of epifauna from destructively sampled tile communities between treatment groups in year two of the thermal manipulation. See Table S3 for treatment codes and abbreviations.

Contrast	Estimate	SE	df	z ratio	P
CC–WC	0.061	0.165	29	0.372	0.982
CC–CW	0.248	0.170	29	1.46	0.472
CC–WW	0.655	0.165	29	3.98	0.0023
WC–CW	0.187	0.170	29	1.10	0.691
WC–WW	0.594	0.165	29	3.61	0.0060
CW–WW	0.407	0.170	29	2.40	0.100

Table S61. Model summary table for Model S29, a generalized linear mixed effects model of the Shannon diversity of epifauna from destructively sampled tile communities collected on 24 February 2021. Shannon diversity was modeled under a Tweedie distribution in relation to the interaction of treatments in year one and year two, with block included as a random effect. Coefficients given are relative to the cool treatment, and the model was tested using a Type III ANOVA. Treatment_{y1} = treatment in year one, treatment_{y2} = treatment in year two, df = degrees of freedom.

Term	Coefficient	SE	χ^2	df	P
Intercept	1.546	0.195			
Treatment _{y1}	-0.251	0.199	1.58	1	0.208
Treatment _{y2}	-0.179	0.233	0.59	1	0.443
Treatment _{y1} * Treatment _{y2}	-0.472	0.305	2.40	1	0.121

Table S62. Tukey-Kramer *post hoc* comparison of the Shannon diversity of epifauna from destructively sampled tile communities between treatment groups in year two of the thermal manipulation. See Table S3 for treatment codes and abbreviations.

Contrast	Estimate	SE	df	z ratio	P
CC–WC	0.251	0.199	35	1.26	0.595
CC–CW	0.179	0.233	35	0.767	0.869
CC–WW	0.902	0.200	35	4.50	0.0004
WC–CW	-0.072	0.228	35	-0.32	0.989
WC–WW	0.651	0.199	35	3.28	0.0121
CW–WW	0.732	0.227	35	3.18	0.0154